Volume 2
Number 10
October 2024
Pages 2719–3154

RSC Sustainability

rsc.li/rscsus

ISSN 2753-8125

ROYAL SOCIETY OF CHEMISTRY

PAPER

James D. Sheehan *et al.*

Glycerol-derived ethers enable hydrogen-free reductive catalytic fractionation of softwood lignin into functionalized aromatic monomers

RSC Sustainability

ROYAL SOCIETY OF CHEMISTRY

PAPER

View Article Online
View Journal | View Issue

Cite this: *RSC Sustainability*, 2024, **2**, 2851

Glycerol-derived ethers enable hydrogen-free reductive catalytic fractionation of softwood lignin into functionalized aromatic monomers†

Bernard C. Ekeoma, Jason E. Bara and James D. Sheehan *

Catalytic reductive processes facilitate deconstruction of lignins into value-added aromatics. This study explores the novel use of glycerol-derived ethers (GDEs), specifically 1-3-dimethoxypropan-2-ol (DMP) and 1,3-diethoxypropan-2-ol (DEP), as hydrogen transfer solvents for reductive catalytic fractionation (RCF) of softwood biomass, marking a departure from conventional use of high-pressure molecular hydrogen and short-chain alcohols. The influence of process conditions, namely, batch holding time, temperature, catalyst species and dosage, solvent-to-biomass ratio, acidic medium (by acetic acid addition), and water volumes as a co-solvent on the yield of aromatic monomers and delignification were evaluated. Under optimal conditions, GDE-mediated RCF of softwood achieved aromatic monomer yields and delignification up to 24.9 wt% and 90.7 wt%, respectively. Aromatic monomers with unsaturated and oxygenated side chains were observed including value-added species, such as vanillin, isoeugenol, coniferaldehyde, eugenol, and vanillic acid. This observation contrasts with prior RCF studies applying *ex situ* hydrogen which yield monomers with saturated alkyl side chains (*e.g.*, 4-propylguaiacol, 4-ethylguaiacol). Mass-based green chemistry metrics (*e.g.*, solvent intensity, process mass intensity) demonstrate GDEs supported material-efficient, catalytic deconstruction of softwood lignins into value-added aromatic monomers. MALDI-TOF analyses of resultant lignin oils revealed the occurrence of sidechain dehydration and decarbonylation of oligomeric species. HSQC NMR of lignin oils indicated the absence of native linkages, especially β-O-4 bonds, post RCF treatment. Furanic monomers derived from carbohydrate fractions were identified and furan yields were higher under neat solvent conditions (~8 wt%) than in the presence of redox catalyst (~2 wt%). This study demonstrated successful and optimized utilization of GDEs as hydrogen transfer solvents for RCF of softwood biomass, resulting in competitive yields of functionalized aromatics within the confines of green chemistry.

Received 4th August 2024
Accepted 19th August 2024

DOI: 10.1039/d4su00441h

rsc.li/rscsus

Sustainability spotlight

Lignin-first biorefineries support sustainable chemical economies by deconstructing lignocellulosic biomass into aromatic chemicals. Reductive catalytic fractionation (RCF) of lignins selectively produces aromatic monomers, albeit requiring the intensive use of volatile solvents and high-pressure hydrogen. Liquid-hydrogen carriers with high boiling points can circumvent the use of hydrogen gas through hydrogen transfer pathways that enable conducting RCF under mild pressures. Sustainable RCF should use hydrogen transfer solvents that are renewable and non-hazardous. The sustainable advancement of our work is evaluating glycerol-derived diethers (GDEs) as eco-friendly, hydrogen transfer solvents to support mild RCF of lignins into value-added aromatics. Overall, our study demonstrates GDE supported RCF of biomass into value-added aromatics under mild conditions. Therefore, our study supports the UN SDG of "sustainable consumption and production".

Introduction

Global demands for energy and chemicals are forecasted to increase by approximately 50% between 2018 and 2050.[1,2] However, chemical manufacturing of organic chemicals is reliant on finite fossil reserves whose procurement and refining have substantial anthropogenic impacts on the environment.[3] Advancing sustainable chemical economies must be realized through development of environmentally cogent methods for refining renewable resources into fuels and chemicals. Lignocellulosic biomass consisting of inedible plant residues has emerged as a promising alternative to fossil resources due to its renewable nature, carbon neutrality, abundant availability, and lack of competition with food production.[4–9] Annual global production of lignocellulosic biomass is estimated at 181.5 Gt, of which only 8.2 Gt are currently utilized, with 7 Gt sourced

Department of Chemical & Biological Engineering, The University of Alabama, Tuscaloosa, AL 35487, USA. E-mail: jdsheehan@ua.edu

† Electronic supplementary information (ESI) available. See DOI: https://doi.org/10.1039/d4su00441h

from forests, agriculture, and grasses and 1.2 Gt from agricultural residues.[10] In a mature market, the United States can produce 1.1 to 1.5 Gt of lignocellulosic biomass annually, providing potential for renewable liquid fuels and chemicals to decarbonize hard-to-abate sectors (*e.g.*, heavy-duty trucking, shipping, aviation, chemicals) and meeting demands for food and environmental services.[11] Future biomass production will primarily rely on purpose-grown energy species, offering a potential annual yield of 300 to 600 Mt.[11] Forestry materials are readily abundant in the US with over 765 million acres of forest, comprising 34% of its total land area.[12] Hardwoods and softwoods that constitute forest resources differ chemically and morphologically, impacting biochemical conversion processes. Both have commercial value, but softwoods dominate production and account for roughly 29 Gt total above ground biomass, with a corresponding biomass density of almost 78 000 tons per mi^2.[13] In order to realize valorization of abundant lignocellulosic biomass, advancements are needed in chemical refining technologies as lignocellulosic materials differ from fossil resources due to their molecular heterogeneity, recalcitrance, and high heteroatom content, in particular oxygen.[4,14,15] Lignocellulosic biomass is constituted by three main biopolymers, namely cellulose (40–60 wt%), hemicellulose (10–40 wt%), and lignin (15–30 wt%).[4,14] Biorefinery processes are primarily based on the valorization of the carbohydrate fraction (*e.g.*, bioethanol production[16,17]). However, economic feasibility and sustainability of lignocellulosic biorefineries can be enhanced by fully integrating the utilization of lignin, which is the most abundant renewable feedstock for aromatic chemicals. Lignin is a polymer of phenylpropane units covalently bonded by approximately 50–70% C–O bonds (*e.g.*, β-O-4) and 30–50% C–C bonds (*e.g.*, β-5, 5–5, and β–β).[18–20] Through selective cleavage of these linkages, lignin can be depolymerized into aromatic compounds with potential applications as feedstocks for liquid fuels, chemicals, and direct use as value-added products (*e.g.*, vanillin). Lignin possesses valuable chemical properties and bioactive effects, and studies indicate that lignin's energy content exceeds the needs of ethanol production.[19] With its robust mechanical, physicochemical, and thermal properties, lignin can be modified for diverse material applications.[6,19] Thus, development of tractable chemical processing technologies is needed to promote scalable integration of lignin-derived products into chemical supply chains.

Reductive catalytic fractionation (RCF) is an emergent thermocatalytic process that can support biorefining of lignin. RCF combines solvothermal extraction of lignin with simultaneous catalytic reductive depolymerization to form aromatic species, including monomers, dimers, and oligomers.[21–23] In comparison to other biorefining technologies, such as organosolv, oxidation, pyrolysis, and hydrothermal liquefaction, RCF offers advantages of high carbon atom economy, better selectivity to monomers, and low char formation.[21–23] RCF of softwood species generally produced monomer yields ranging 10–30 wt% and delignification ranging 40–95 wt%.[22,24–33] Common solvents include short chain alcohols such as methanol, ethanol, and isopropyl alcohol, and catalysts consist primarily of supported noble metals and Ni nanoparticles.[21–23,34,35] However, a major limitation of RCF is utilization of high-pressure molecular hydrogen (10–50 bar),[6,24] which necessitates the use of capital intensive and specialized high-pressure reactors to mitigate safety risk factors. Liquid-hydrogen carriers can circumvent the need for *ex situ* hydrogen and offer routes for applying "green" hydrogen derived from bio-based chemicals, such as formic acid and alcohols.[36–38] As such, hydrogen transfer solvents consisting of liquid-hydrogen carriers can support *ex situ* H_2-free RCF of lignins. However, elevated pressure conditions (>20 bar) still exist owing to the high volatility of predominantly used short-chain (*i.e.*, low boiling point) alcohols.[39–42] Tractable low-pressure and H_2-free RCF processes should use non-volatile and renewable chemicals as hydrogen transfer solvents.

Non-volatile compounds have garnered research interest as hydrogen transfer solvents to facilitate hydrogenation reactions in biomass conversion processes.[43–45] Through utilizing non-volatile hydrogen carriers, the need for high-pressure storage and transportation infrastructure for molecular hydrogen can be circumvented. Amongst non-volatile, hydrogen transfer solvents, glycerol has gained attention due to its abundance, low-cost, and renewability.[46,47] O'Dea *et al.* performed a reactive-distillation process for H_2-free RCF of technical lignins using glycerol at 250 °C and reported aromatic monomer yields of 31.7 wt%.[48] Facas *et al.* conducted H_2-free RCF of poplar using glycerol at 225 °C with several heterogeneous catalysts and reported aromatic monomer yields ranging from approximately 5 to 10 wt%.[49] Furthermore, the same authors evaluated glycols (*e.g.*, ethylene glycol, propylene glycol, butylene glycol) for H_2-free RCF and reported aromatic monomer yields ranging from approximately 11 to 20 wt%. Collectively, these results indicate the promising efficacy of non-volatile, hydrogen transfer solvents for H_2-free RCF of lignins. Nonetheless, the viscosities of glycerol (1412 mPa s) and glycols (~18 to 50 mPa s) lead to challenges with downstream processability and separation; indeed, processing limitations of glycerol (*i.e.*, very high boiling point and viscosity) contributed to its designation as a "problematic" solvent in the CHEM21 solvent selection guide.[50] Furthermore, biorefining solvents should consist of "benign" species derived from renewable resources, in accordance with green chemistry principles.[51] For instance, ethylene glycol and its oligomers (mono-, di-, tri-, tetra-, and penta-ethylene glycol) are acutely toxic at high concentrations and rapidly absorbed through ingestion and inhalation.[52] Additionally, despite promising efforts made towards shifting to biomass-derived ethylene glycol, industrially, it is produced primarily *via* hydration of ethylene oxide, which is itself derived from petrochemicals (*e.g.*, ethylene).[53] As such, efforts towards advancing eco-friendly and biogenic solvent candidates could support sustainable biorefining of lignins.

Hence, in the present study, we investigate the novel use of glycerol-derived ethers (GDEs) as hydrogen transfer solvents to support extraction and catalytic hydrogenolysis of softwood lignin into value-added aromatics. GDEs are produced through etherification of glycerol scaffolds with alcohols, leading to production of bio-derived solvents with elevated boiling points (~160 to 200 °C) and modest viscosities (~3 to 4 mPa s at 20 °C), which, collectively, can support development of tractable low-

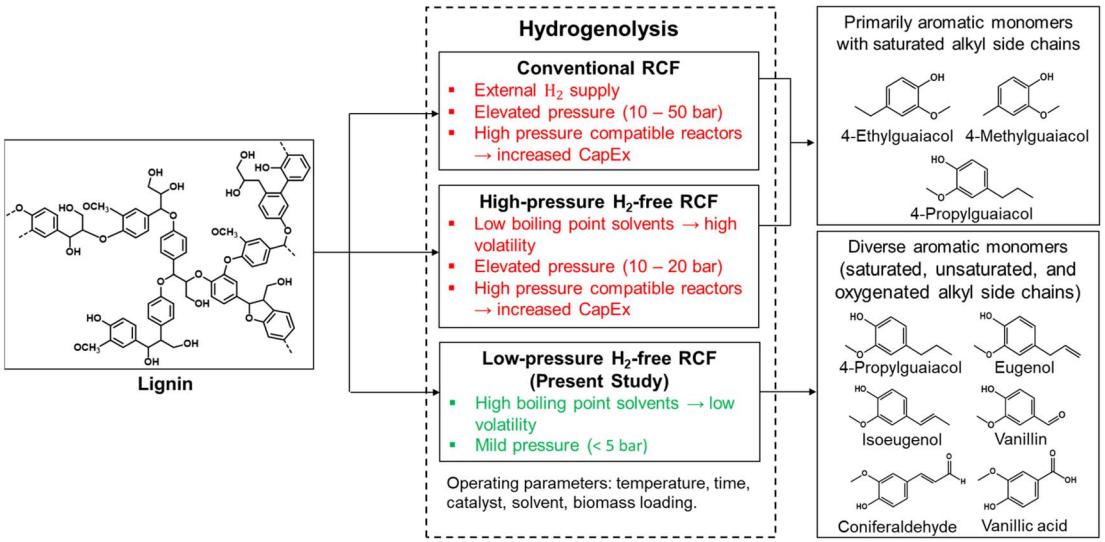

Scheme 1 Illustration of how this study (low pressure H_2-free RCF) offers significant advancements in process safety, sustainability, and product range when compared to traditional RCF and high pressure H_2-free RCF.

pressure and H_2-free RCF processes. GDEs have been evaluated previously for plastic upcycling[54–56] and CO_2 absorption.[57–59] However, their application towards biomass valorization has not been evaluated. Thus, we evaluate application of two GDEs, specifically, 1-3-dimethoxypropan-2-ol (DMP, 170 °C, 3.52 mPa s) and 1,3-diethoxypropan-2-ol (DEP, 188 °C, 3.93 mPa s)[54,57,60] as hydrogen transfer solvents for H_2-free RCF. The influence of process conditions on monomer yields and delignification was evaluated, specifically, effects of time, temperature, catalyst dosage, and solvent-to-biomass ratio. Furthermore, the influence of employing water as a co-solvent and addition of organic acid additives was explored. A series of chromatographic and spectroscopic techniques were employed to characterize liquid and solid products, in order to provide insights into the depolymerization process. With increasing demand for sustainable chemicals produced by environmentally benign processes, GDEs can support advancement of green solvents that drive lignin deconstruction towards value-added chemicals. By leveraging GDEs as hydrogen transfer solvents for H_2-free RCF, this study promotes green chemistry principles including the use of less hazardous chemical syntheses, safer solvents and auxiliaries, the use of renewable feedstock, and inherently safer chemistry for accident prevention.[51] Distinctions of the present study with respect to the state of the art are offered in Scheme 1.

Experimental section

Chemicals

No additional purification was conducted on the commercially purchased chemicals used in this study. Ruthenium on carbon (Ru/C, 5 wt% Ru) and platinum on carbon (Pt/C, 5 wt% Pt) catalysts were purchased from BeanTown Chemical Corporation. Pure phenolic monomers were used as calibration standards for GC-FID quantification, specifically 2-methoxy-4-propylphenol (4-propylguaiacol), 2-methoxy-4-ethylphenol (4-ethylguaiacol), 3-(4-hydroxy-3-methoxyphenyl)prop-2-enal (coniferaldehyde), 2-methoxy-4-(2-propenyl)phenol (eugenol), 2-methoxy-4-((*E*)-prop-1-enyl)phenol (*trans*-isoeugenol), 4-hydroxy-3-methoxybenzaldehyde (vanillin), and 4-hydroxy-3-methoxy-benzoic acid (vanillic acid) were purchased from Sigma-Aldrich (all ≥98%). Acetic acid (AA, ≥99.7%) and acetone (≥99.5%) were purchased from VWR, dimethylsulfoxide-d_6 (99.8%) and heptane (99%) from Sigma-Aldrich, dichloromethane (DCM, ≥99.5%) from Macron Fine Chemicals, and isopropyl alcohol (iPrOH, ≥99.5%) from J. T. Baker. Ultrapure water was obtained from a Milli-Q® IQ 7005 (Q-Pod dispenser). For chemicals used in the synthesis of the GDEs, (±)-epichlorohydrin (ECH, 99%) and sodium sticks (99%, in mineral oil) were respectively procured from BeanTown Chemical and Alfa Aesar, ACS-grade methanol (MeOH) and ethanol (EtOH) were purchased from VWR, and anhydrous magnesium sulfate ($MgSO_4$, >99.8%) was purchased from JT Baker.

Synthesis of glycerol-derived ethers

The syntheses of DMP and DEP were performed in accordance with the methods published by Qian *et al.*[57] To produce DMP, a 1000 mL round-bottom flask was used, and 300 mL of MeOH (237.6 g, 7.42 mol) was added to the flask under careful temperature control at 0 °C using a circulating chiller. Sodium metal (24.15 g, 1.05 mol) was carefully added in portions over 30 min. The reaction mixture was then transferred to a hotplate and heated to 50 °C until all sodium particles disappeared. ECH (46.26 g, 0.50 mol) was added dropwise over 30 min, and the reaction was stirred overnight at 50 °C with a reflux condenser attached. Afterward, the reaction was quenched with 50 mL of deionized water. Any remaining MeOH was removed using rotary evaporation. DCM (300 mL) was added to the remaining liquid in the flask. The organic phase was washed with 5 × 50 mL of deionized water and dried using anhydrous $MgSO_4$. The solids were filtered, and DCM was removed *via* rotary

evaporation. The resulting product was then distilled and stored over molecular sieves. The isolated yield was 31.23 g (52.0%). The 1H NMR analysis (500 MHz, DMSO-d_6) showed peaks at δ 4.77 (d, J = 5.2 Hz, 1H), 3.74–3.67 (m, 1H), 3.29 (dd, J = 9.9, 4.9 Hz, 2H), and 3.27–3.20 (m, 8H). These ^{1}H NMR results were consistent with the literature.[60]

DEP was obtained through a reaction involving EtOH (300 mL, 236.7 g, 5.14 mol), ECH (46.26 g, 0.50 mol), and sodium (24.15 g, 1.05 mol) using a similar approach to the synthesis of DMP. The isolated yield was 41.32 g (55.8%). The 1H NMR analysis (500 MHz, DMSO-d_6) showed peaks at δ 4.71 (d, J = 5.2 Hz, 1H), 3.69 (qd, J = 5.8, 5.0 Hz, 1H), 3.47–3.39 (m, 4H), 3.33 (dd, J = 9.9, 5.1 Hz, 2H), 3.27 (dd, J = 9.7, 6.0 Hz, 2H), and 1.10 (td, J = 7.0, 0.7 Hz, 6H). These ^{1}H NMR results were consistent with the literature.[60]

Biomass preparation

Moisture, extractives, ash, lignin and holocellulose contents (mass fractions) of lodgepole pine (LPP) were determined in a previous study[61] following the Laboratory Analytical Procedures of the National Renewable Energy Laboratory (NREL).[62–64] In brief, LPP chips sized at ≤2 mm underwent a drying process in a vacuum oven at 105 °C for 15 h until a consistent mass was achieved. The moisture content of the chips was determined by dividing the mass of the dried chips by the mass of the chips before drying. Extractives were removed *via* Soxhlet extraction using EtOH and resulting extract-free biomass was subjected to washing, filtration, and drying to produce dried extract-free pine (DEFP). Oil isolated from the extraction process was considered extractives. Ash content was determined by heating the moisture-free chips in a muffle furnace and quantifying the weight of the resultant ash. The Klason lignin analysis method was employed to quantify lignin content of the DEFP, as described in Section A of the ESI.† Holocellulose content was calculated as the difference between unity and the Klason lignin content. Relevant equations and results for these analyses are presented in Table S2.†

H_2-free reductive catalytic fractionation

H_2-free RCF experiments were carried out in 15 mL heavy-wall, borosilicate tube reactors (Ace Glass). 730 mg of biomass (DEFP) were carefully loaded into the reactors followed by the catalyst (0.1–0.3 g cat per g DEFP), solvent (0.0068, 0.0096, 0.0137, and 0.0205 mL per mg DEFP), and a magnetic stir bar. Reactors were sealed with a Teflon screw cap and placed into a preheated oil bath with a mixing rate of 1000 rpm. Variations in the process solvent composition, reaction temperature (160–250 °C), time (1–7 h), catalyst dosage and solvent-to-DEFP ratio were employed to achieve optimal results. Variations in process solvent composition included the use of either neat 7 mL GDE, 7 mL GDE + AA as an additive (0.5, 0.6, and 0.7 g AA per g DEFP), 1 : 1 vol GDE/vol H_2O, and finally 1 : 1 vol GDE/vol H_2O with an AA additive loading of 0.6 g AA per g DEFP. Control experiments including RCF in the absence of the catalyst and 1 : 1, 1 : 5 and 2 : 1 v/v glycerol/H_2O solvents were also performed. Reactions were primarily conducted with the reactor headspace composed of air; however, control experiments using an inert gas (*e.g.*, 1 atm He) were also implemented. After completing a set reaction time, the reaction was quenched by allowing the reactor to cool to room temperature. Vacuum filtration was used to separate the resulting black liquor (BL) from residual pulp, after which the pulp was washed with 10 mL isopropanol, 10 mL acetone and 5 × 10 mL ultrapure water before drying for 12 h at 105 °C in an oven. Pulp yield was calculated using eqn (1). The Klason method of lignin analysis was subsequently employed in determining the lignin content of the residual pulp, and delignification was calculated using eqn (2). Concern about pulp yield overestimation due to the presence of catalyst particles in the isolated pulp was resolved using Energy-Dispersive X-ray Spectroscopy (EDS). The result of EDS analysis revealed a negligible presence of the catalyst metal in the pulps and is provided in Section A of the ESI.† Liquid–liquid extraction (LLE) (to remove soluble sugars) and micro-distillation unit operations (to remove GDEs) were carried out on the BL to yield the desired depolymerized lignin oil (LO). Details of the Klason lignin determination, LLE and micro-distillation are provided in Section A of the ESI.†

$$\text{Pulp yield(wt\%)} = \frac{\text{mass of dried residual pulp}}{\text{mass of DEFP}} \times 100 \quad (1)$$

$$\text{Delignification(wt\%)} = \left(1 - \frac{\text{mass of acid insoluble lignin in dried residual pulp}}{\text{mass of insoluble lignin in DEFP}}\right) \times 100 \quad (2)$$

Surface morphology characterization by scanning electron microscopy

Surface morphology characterization of solid samples was carried out using an Apreo 2 ThermoFisher Scientific scanning electron microscope (SEM). Initially, wood chips and residual pulp samples underwent a gold coating process to enhance their conductivity. Coating was performed using an MCM-200 Ion Sputter Coater from Micro-Optics by applying a current of 10 mA for 2 min. Subsequently, SEM imaging was performed using an ETD detector in the secondary electron (SE) mode, employing low voltage (2.00 kV) and low current (3.1 ρA) settings to prevent sample incineration. Working distance (WD) and scanning resolution were set to 10 mm and 1536 × 1024, respectively, and imaging was conducted at magnifications ranging from 50× to 500×. The EDS spectrum was collected under the same conditions with the counts per second (cps) being above 9×10^3.

Crystallographic characterization by X-ray diffraction (XRD)

Crystallinity of fresh DEFP and RCF pulps was evaluated using a Rigaku MiniFlex desktop X-ray diffractometer in the 2θ range between 5° and 50°. Cu Kα radiation, a high voltage of 623.5 V, a scan rate of 2° min^{-1}, and a width of 0.05° were used. Size reduction with a mortar and pestle was done prior to XRD analysis.

Identification of lignin monomers by GC-MS

Samples for GC-MS were prepared using a 1 : 20 dilution ratio of LO/heptane, after which the mixture was vortexed. Analysis was conducted using an Agilent 7890 A series gas chromatograph (GC) equipped with an HP5-MS capillary column measuring 30 m (length) and 0.32 mm (internal diameter, i.d.) and with a 0.25 μm film thickness. An Agilent 5975C inert XL MSD with a Triple-Axis detector was employed, with helium serving as the carrier gas. Initial and injection temperatures were 40 °C and 250 °C respectively, the ramp rate was 25 °C min^{-1}, and final temperature was 300 °C with a hold time of 5.6 min. After analysis, species associated with individual peaks were identified by matching peak mass spectra and total ion chromatogram (TIC) values to standard reference values in the National Institute of Standards and Technology (NIST) database.

Quantification of lignin monomers by GC-FID

Samples for GC-FID were prepared using a 1 : 20 dilution ratio of LO/DCM, and 1 μL iPrOH was used as an internal standard (IS). Analyses were performed on a Thermo Scientific Trace 1310 GC equipped with a 30 m × 0.25 × 0.25 (length × internal diameter × film thickness) Rtx-5 column and a flame ionization detector (FID) using helium as carrier gas. Both injection and detection temperatures were 300 °C. The column temperature program consisted of an initial temperature of 30 °C, ramping at a rate of 10 °C min^{-1} to 340 °C and holding at 340 °C for 4 min. Lignin monomer yield (total lignin basis), monomer selectivity, and monomer productivity were calculated with eqn (3) and (4) respectively.

$$\text{Monomer yield(wt\%)} = \frac{\text{mass}_{\text{monomer}}}{\text{mass}_{\text{DEFP,initial}} \times \text{DEFP initial lignin content}} \times 100 \quad (3)$$

$$\text{Monomer selectivity}_{\text{exp.i}} = \frac{\text{total monomer yield(wt\%)}_{\text{exp.i}}}{\text{delignification(\%)}_{\text{exp.i}}} \quad (4)$$

Molecular weight characterization of LO samples using MALDI-TOF

Molecular weights of the deconstructed lignins were evaluated using a Bruker RapifleX MALDI-TOF/TOF & MALDI imaging spectrometer. Red phosphorus (P-red) was used for calibration, MS thin layer laser application was used, and MS were recorded in the linear positive ion mode using 2,5-dihydroxybenzoic acid as the matrix. To improve the signal-to-noise ratio and accuracy, spectral averaging was done after replicate spotting at different points. Analysis of generated spectra was done using RapifleX Flexcontrol/FlexAnalysis software.

Structural elucidation of depolymerized lignins by ^{1}H–^{13}C HSQC NMR and ^{1}H NMR

^{1}H–^{13}C HSQC NMR and ^{1}H NMR spectroscopies were conducted to evaluate the molecular structures of the RCF lignins. Samples were prepared for NMR analysis as follows: 50 μl of LO (73 mg) was dissolved in 500 μl of DMSO-d_6 and transferred into an NMR test tube. LO samples were recorded at 25 °C on an Avance 500 NMR spectrometer (Bruker) with an Oxford Cryomagnet (74 × 40 × 40 in), equipped with a BBI inverse broad band probe with z-gradients, a BVT3000 unit for temperature control, and a low T accessory. With regard to the analysis settings, Bruker standard pulse sequence 'hsqcetgpsp.3' was employed, utilizing the following parameters: a spectral width of 13 ppm with 2048 data points in the F2 dimension (^{1}H), a spectral width of 165 ppm with 256 data points in the F1 dimension (^{13}C), and a total of 16 scans recorded with a 2 s interscan delay (D1).[23] ^{1}H NMR data processing was performed using the MestReNova software, while TopSpin 4.3.0 data processing software was used for HSQC NMR. Chemical shifts were referenced to the central DMSO peak (δ_C/δ_H 39.5/2.5 ppm) and assignment of the HSQC spectra was based on previously reported spectra.[65,66]

Results and discussion

The following section provides an in-depth presentation and explanation of the results obtained from this study. First, GDEs are evaluated for H_2-free RCF of softwood biomass in the presence of heterogeneous catalysts. Secondly, the influence of process conditions on delignification and aromatic monomer yields is evaluated. Thirdly, molecular characterization of the deconstruction lignins is elucidated with MALDI-TOF and NMR analyses. Finally, characterization of the residual pulps and furan monomers is conducted to gain insights into the impact of the H_2-free RCF process on holocellulose. Tabulated versions of the data presented in this study are offered in the SI.

Influence of solvent and catalyst on H_2-free RCF

Fig. 1a offers results for monomer yield, delignification, and pulp yield resulting from H_2-free RCF using DMP, DEP, and aqueous glycerol solvents. Glycerol was evaluated as a benchmark for GDEs, and aqueous glycerol solutions were evaluated due to difficulty in working up viscous glycerol liquors. RCF was conducted at 200 °C for 7 h with 10 wt% catalyst (5 wt% Pt/C) loading. For clarification, monomer yields and delignification are based on the initial lignin content of DEFP (0.289 g lig. per g DEFP), while pulp yields are based on the total DEFP mass. Dried pulp yields were found to be highest when using aqueous glycerol mixtures, ranging from 43.6–44.8 wt%. GDEs produced lower pulps as DMP and DEP resulted in yields of 34.4 wt% and 36.3 wt%, respectively. Correspondingly, DMP and DEP facilitated higher degrees of delignification, 79.1 wt% and 75.2 wt%, respectively, while values for aqueous glycerol mixtures ranged from 58.7–63.7 wt%. RCF using DMP produced the highest monomer yield, 22.9 wt%, while DEP yielded 21.4 wt%. Aromatic monomer yields were not reported for the aqueous glycerol mixtures as their viscosity inhibited successful work up of the product matrix to isolate liquid products derived from lodgepole pine. This observation buttresses earlier motivations for evaluating glycerol derivatives as RCF solvents.[28,67–69] The observed

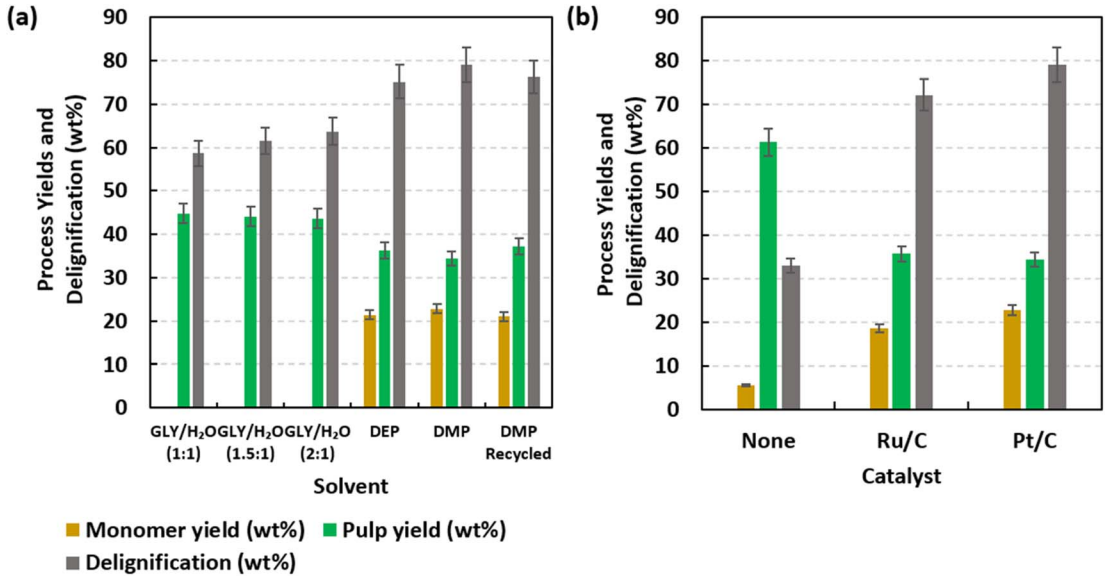

Fig. 1 Total monomer yield, pulp yield, and delignification with respect to speciation of (a) solvent (Pt/C as the catalyst) and (b) catalyst (DMP as solvent). Reaction conditions: 730 mg DEFP (595 mg in the experiment with recycled DMP), 7 mL solvent (5.7 mL recovered and used in the DMP recycle experiment), 73 mg catalyst (59.5 mg for DMP the recycle experiment), 200 °C, 7 h, 0.1 g per g catalyst dosage, 0.0096 mL per mg solvent-to-DEFP ratio, 1000 rpm.

yields of aromatic monomers are comparable with those reported for conventional and hydrogen-transfer RCF, which demonstrates the efficacy of DMP and DEP as solvents for H_2-free RCF. Fig. 1b provides the influence of heterogeneous catalysts on monomer yield, delignification, and pulp yield. Specifically, RCF was conducted at 200 °C, 7 h, 0 wt% or 10 wt% catalyst loading with DMP as solvent. With respect to aromatic monomer yield and delignification, in decreasing order, catalytic systems ranked as Pt/C > Ru/C > no catalyst. When pulp yield is considered, the opposite ranking occurs. Pt/C facilitated a monomer yield and delignification of 22.9 wt% and 79.1 wt%, respectively, while Ru/C facilitated respective values of 18.6 wt% and 72.1 wt%. In the absence of the catalyst, lower monomer yield and delignification, 5.5 wt% and 33.0 wt%, respectively, were observed. Interestingly, formation of monomers in experiments devoid of catalysts indicates that GDEs can facilitate solvolysis of interunit linkages present in lignin. Furthermore, higher degrees of delignification were observed for heterogeneous catalytic systems, which potentially indicates that deconstructed lignins support solubilization of lignins within lignocellulosic substrates.[70–74]

As indicated in Fig. 1a, DMP acted as the optimal solvent as it is associated with higher monomer yields and delignification. Efficacy of DMP could be attributed to factors including favorable solubility of lignins and electronic effects facilitated by the terminal methoxy groups that promote hydrogen abstraction. Solubility effects are investigated using Hasen solubility parameters (HSPs), as presented in Table S3;† HSP values for a wide range of GDEs were recently reported by Soyemi and Szilvási.[54] In comparison to DEP, HSPs of DMP align more closely with values reported for lignin[75] and monolignols,[76] thus indicating that their intermolecular forces are relatively well-matched and may effectively associate. Furthermore, methoxy groups are smaller than ethoxy and experience less steric hindrance,[77] thus enabling increased molecular accessibility to extract lignins from mesoporous wood structures. This observation is corroborated by our previous study that demonstrated an inversely proportional relationship between molecular volume of solvents and delignification of softwoods.[61] Considering the need for sustainability and enhancing overall solvent intensity, the recyclability of GDEs was investigated by conducting H_2-free RCF with recycled DMP under the same experimental conditions (200 °C, 7 h, 10 wt% loading of 5 wt% Pt/C, and 0.0096 mL per mg solvent-to-DEFP ratio) used in the experiment with fresh DMP. This is presented in the last set of columns in Fig. 1a. Monomer yield, pulp yield, and delignification obtained were respectively 21.03 wt%, 37.22 wt%, and 76.3 wt%; these outcomes were very similar to those observed using fresh DMP. This result demonstrates that GDEs have excellent potential for solvent recycling and reusability to further facilitate additional iterations of RCF.

Fig. 2 provides speciation of aromatic monomers produced by neat solvolysis (*i.e.*, no catalyst) and H_2-free RCF. Neat solvolysis of DEFP using GDEs produced vanillin and coniferaldehyde as major monomer products. In the presence of heterogeneous catalyst, yields of monomer species increased along with a diversification of the product profile. For instance, in the presence of the catalyst, major monomer species included vanillin, vanillic acid, *trans*-isoeugenol, eugenol, coniferaldehyde, 4-ethylguaiacol, and 4-propylguaiacol. Interestingly, selectivity favored highly functionalized lignin monomers, consisting of carbonylated and unsaturated side chains, which is a unique outcome of the present RCF study. Fig. S1† shows the selectivity for dominant monomeric species under neat solvolysis and H_2-free RCF. Previous RCF studies

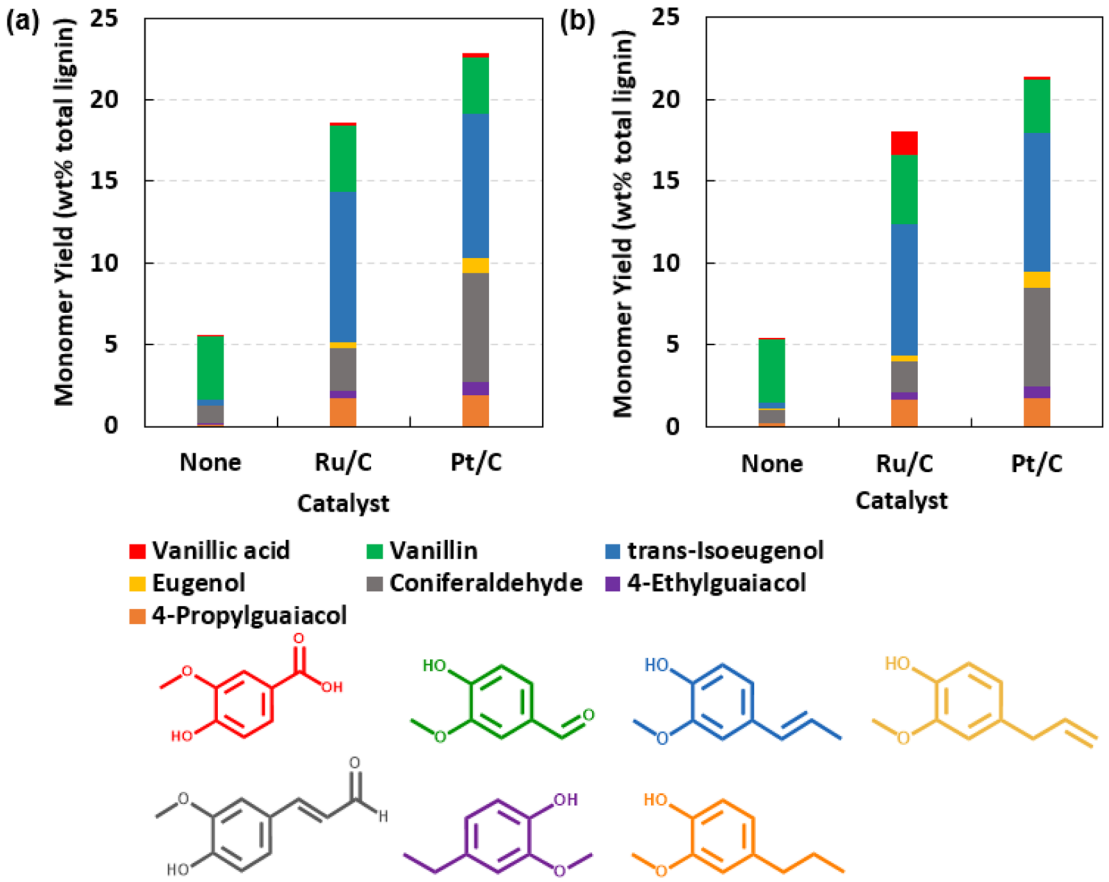

Fig. 2 Monomer yields (lignin mass basis) resulting from H_2-free RCF of DEFP with (a) DMP and (b) DEP. Reaction conditions: 730 mg DEFP, 7 mL solvent, 200 °C, 7 h, 0.1 g cat. per g DEFP, 0.0096 mL solvent per mg DEFP, 1000 rpm.

leveraging *ex situ* H_2 predominately produced lignin monomers containing saturated alkyl side chains (*e.g.*, propyl, ethyl).[21–23,26] More recent studies pursuing H_2-free RCF with non-volatile solvents have reported the presence of lignin monomers with alkenyl side chains, although in low abundance;[48,49] lignin aromatic compounds with carbonylated side chains were not reported. However, formation of aromatics with oxygenated side chains has been reported previously for solvolytic processes (*e.g.*, Hibbert ketones).[78,79] Interestingly, several of the resultant monomers in the present studies have direct economic value as fragrances and flavorants, including vanillin, eugenol, and coniferaldehyde, which could enable an insertion point into high-value marketspaces. Overall, these observations indicate unique capacities of GDEs as hydrogen transfer solvents for enabling product selectivities towards functionalized and value-added aromatics.

Mechanistic origins of the lignin monomers with oxygenated side chains were probed by evaluating the role of the gaseous species comprising the headspace by benchmarking reactions conducted under an air headspace (standard procedure) against those run under an inert gas (*e.g.*, helium). Interestingly, RCF conducted under inert headspace resulted in lignin monomer yields (22.3 wt%) and product selectivities comparable to those produced in air headspace under comparable conditions (200 °C, 7 h, 10 wt% catalyst; see Table S5 in the ESI†). This observation indicates that in the present system, autoxidative routes do not facilitate formation of oxygenated lignin monomers. We hypothesize that oxygenated lignin monomers are produced *via* solvolytic routes akin to Hibbert ketones[78,79] and subsequently, reactive intermediates are quenched *via* reduction on the catalyst surface. In comparison to conventional RCF using *ex situ* H_2, we hypothesize that the catalyst surface in the present system is relatively hydrogen poor, thus enabling production of oxygenated lignin monomers rather than those with fully saturated sidechains.

Effects of process conditions on H_2-free RCF

Fig. 3 presents the influence of RCF conditions on monomer yields, delignification, and dried pulp yields. Specifically, the influence of process conditions such as temperature, time, catalyst dosage, and solvent-to-DEFP ratio was evaluated. Given their optimal performances observed previously (Fig. 1), DMP and Pt/C were employed as solvent and catalyst, respectively. Fig. 3a provides aromatic monomer yield, delignification, and pulp yield resulting from H_2-free RCF conducted for 4 h with 10 wt% catalyst at varying temperatures. Monomer yield increased from 16.1 wt% to 20.3 wt% as temperature was varied from 160 °C to 200 °C. Temperatures above 200 °C promoted small changes in monomer yield; for example, aromatic

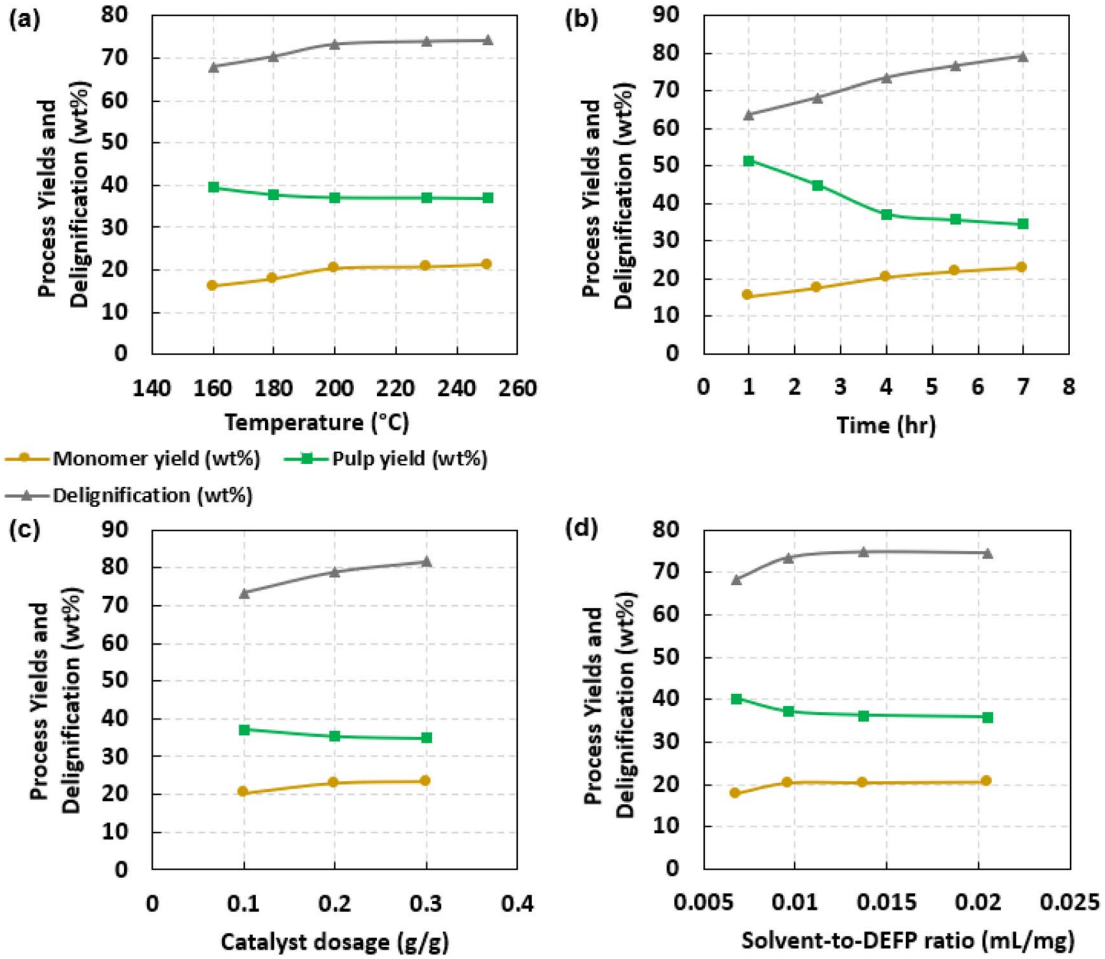

Fig. 3 Effects of (a) temperature, (b) time, (c) catalyst dosage, and (d) solvent-to-DEFP ratio on monomer yield (yellow), delignification (gray), and dried pulp yield (green). Reaction conditions: 730 mg DEFP, 7 mL DMP, 73 mg 5 wt% Pt/C, 200 °C (b–d), 4 h (a, c and d), 0.1 g per g catalyst dosage (a, b and d), 0.0096 mL per mg solvent-to-DEFP ratio (a–c), 1000 rpm.

monomer yields at 230 °C and 250 °C were 20.7 wt% and 21.2 wt%, respectively. Delignification increased from 67.9 wt% to 73.4 wt% as temperature was increased from 160 °C to 200 °C. Delignification followed a similar trend to the aromatic monomer yields, whereby increasing temperature beyond 200 °C had little impact; for instance, H_2-free RCF conducted at 250 °C led to a delignification of 74.3 wt%. Pulp yield reduced from 39.5 wt% to 37.2 wt% as temperature was increased from 160 °C to 200 °C, followed by negligible drops to 37.1 wt% and 37.0 wt% with a further increase in temperature to 230 °C and 250 °C, respectively. Collectively, these observations indicate that 200 °C is an optimal temperature for DMP-mediated, H_2-free RCF of softwood biomass. These trends are consistent with those of previous RCF, where significant increments in the yields of desired products were primarily observed at temperatures below 230 °C. Beyond this temperature, increased increments had negligible effects on product yields.[22,24–33]

Fig. 3b demonstrates the influence of batch holding time on aromatic monomer yield, delignification, and pulp yield resulting from RCF. These experiments were conducted at 200 °C with 10 wt% catalyst and varying batch holding times. Increasing the reaction time from 1 h to 7 h led to increasing monomer yield (15.3 to 22.9 wt%) and delignification (63.7 to 79.1 wt%) and decreasing pulp yield (51.3 to 34.4 wt%). These trends are consistent with those in previous reports as increasing process intensity led to higher product yields and deconstruction of biomass.[22,26,80,81]

Fig. 3c offers insight into the influence of catalyst dosage on H_2-free RCF. RCF was conducted at 200 °C for 4 h, with varying catalyst dosages. An increase in catalyst dosage from 0.1 to 0.3 g cat. per g DEFP resulted in an increase in monomer yield (20.3 to 23.3 wt%) and delignification (73.4 to 81.7 wt%). However, monomer yield and delignification achieved with 0.2 g cat. per g DEFP were similar to those resulting from 0.3 g cat. per g DEFP. This trend indicates that a further increase in catalyst dosage beyond 0.2 g cat. per g DEFP has a negligible impact on monomer yield and delignification. Similarly, for pulp yield, an increase in catalyst dosage from 0.1 to 0.3 g catalyst per g DEFP resulted in a decrease in the value from 37.2 wt% to 35.0 wt%; pulp yields at 0.2 g cat. per g DEFP and 0.3 g cat. per g DEFP were comparable.

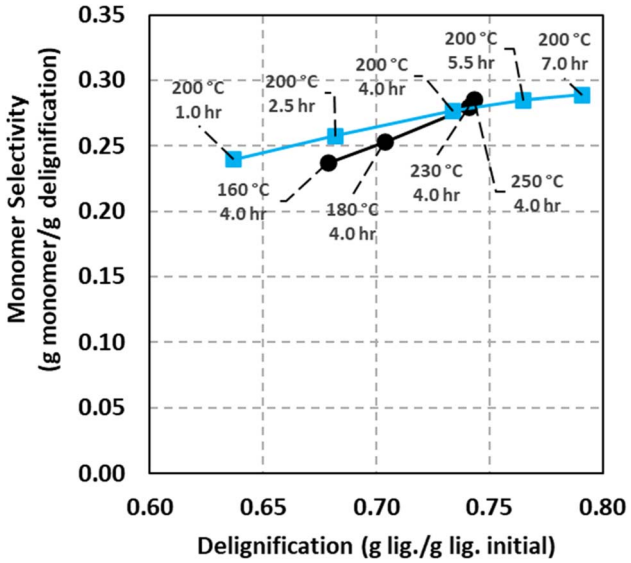

Fig. 4 Lignin extraction and monomer production relationship for temporal (blue, 200 °C) and temperature variations (black, 4 h). Reaction conditions: 730 mg DEFP, 7 mL DMP, 73 mg Pt/C, 0.1 g per g catalyst dosage, 0.0096 mL per mg solvent-to-DEFP ratio, 1000 rpm.

Fig. 3d provides the influence of the solvent-to-DEFP ratio on H_2-free RCF. These experiments were conducted at 200 °C for 4 h and used 10 wt% catalyst. Experiments were conducted by fixing DEFP to a mass of 730 mg and varying the volume of DMP from 5 mL (0.0068 mL DMP per mg DEFP) to 7 mL (0.0096 mL per DMP mg DEFP). Overall, increasing solvent loading from 0.0068 to 0.0096 mL DMP per mg DEFP led to an increase in monomer yield (17.8 to 20.3 wt%) and delignification (68.5 to 73.4 wt%). Enhancements in monomer yield and delignification by increasing solvent loading can be attributed to enhanced mass transfer, increased availability of hydrogen transfer sources, and better catalyst dispersion. A further increase in solvent loading did not facilitate appreciable improvements as 0.0205 mL per DMP mg DEFP produced a monomer yield and delignification of 20.5 wt% and 74.5 wt%, respectively. Similar trends were observed with respect to the decrease in pulp yield as solvent loading increased.

Relationships between the extent of delignification and monomer selectivity were evaluated in an analogous fashion as classic conversion *versus* selectivity plots, as shown in Fig. 4. In this analysis, monomer selectivity is defined as the ratio of mass of lignin monomers and the mass of lignin removed from the softwood feedstock (*i.e.*, yield divided by conversion). Two experimental cases were considered: isothermal conditions (200 °C) with temporal variations and constant batch holding time (4 h) with temperature variations. In both cases, as delignification increases from approximately 0.63 to 0.78 g per g lig. initial, selectivity for monomers increases from approximately 0.24 to 0.29 g mon. per g delig. A monotonic increase in a given product selectivity in conversion *versus* selectivity plots indicates that the product is terminal with respect to the global reaction network. Under this interpretation, Fig. 4 suggests that aromatic monomers are terminal products within the evaluated reaction system. This observation is operationally significant as lignin-derived aromatics are known to be reactive towards recondensing into higher molecular weight products, especially in the presence of Brønsted acids or electron-deficient intermediates (*e.g.*, carbocations). Thus, the delignification *versus* monomer selectivity plot indicates that GDE solvent systems support stabilization of aromatic monomers and may limit their selectivity towards formation of higher molecular weight products. The present analysis was conducted in a limited range of delignification values, and future experiments should consider careful evaluation of delignification *versus* monomer selectivity trends under a wider range of delignification conditions.

Influence of organic acid additives and aqueous co-solvent

Fig. 5a demonstrates the effect of introducing organic acid additives (*e.g.*, AA) to H_2-free RCF. Integrating AA was of interest

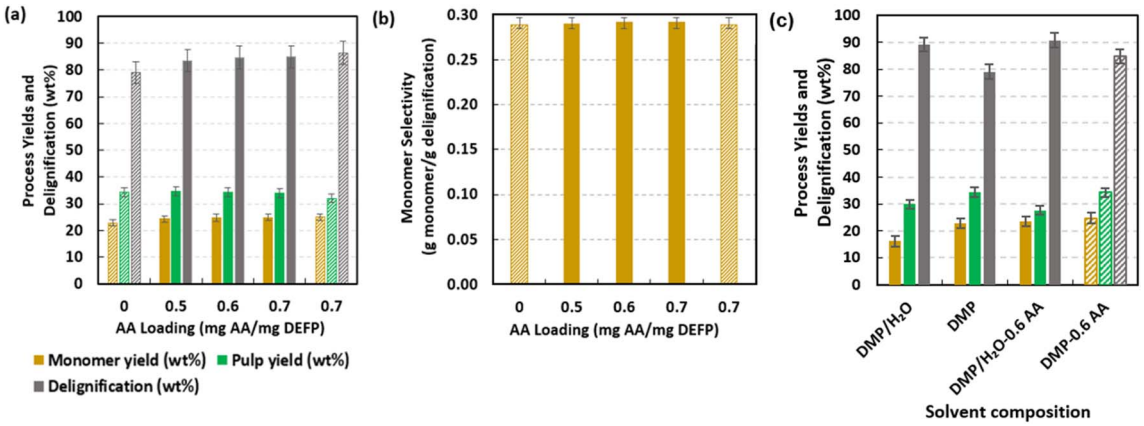

Fig. 5 (a) Influence of organic acid additive (AA) on H_2-free RCF process yields. (b) Monomer selectivity of H_2-free RCF experiments with the AA additive. Reaction conditions associated with Fig. 5 (a and b): 730 mg DEFP, 7 mL DMP, 73 mg Pt/C, 200 °C, 4 h (bars not hatched), 7 h (hatched bars), 0.1 g per g catalyst dosage, 0.0096 mL per mg solvent-to-DEFP ratio, 1000 rpm. (c) Influence of using water as a co-solvent on H_2-free RCF process yields. Reaction conditions associated with (c): 730 mg DEFP, 7 mL DMP, 73 mg Pt/C, 200 °C, 4 h (hatched bars), 7 h (bars not hatched), 0.1 g per g catalyst dosage, 0.0096 mL per mg solvent-to-DEFP ratio, 1000 rpm.

as organic acids have precedent for increasing lignin extraction in organosolv processes.[82–84] This study was conducted at 200 °C for 4 and 7 h, using a heterogeneous catalyst dosage of 10 wt%. Increasing the presence of AA led to higher monomer yields and delignification, thus indicating that organic acid additives promote lignin extraction and deconstruction. This observation is consistent with Renders *et al.*; however, these authors applied a stronger acid (*e.g.*, H_3PO_4) which led to larger relative increases in yields.[25] For a 4 h reaction, monomer yield increased from 22.9 wt% (no AA, 7 h) to 24.3 wt% (0.5 mg AA per mg DEFP). A further increase to 0.6 and 0.7 mg AA per mg DEFP led to limited increments in monomer yields, 24.7 wt% and 24.8 wt%, respectively. Extending the 0.7 mg AA per mg DEFP loading experiment to 7 h led to a negligible monomer yield increase (24.9 wt%). In the 4 h experiments, delignification showed an increase from 79.1 wt% (without AA) to 83.5 wt% (0.5 mg AA per mg DEFP). Subsequent increases to 0.6 and 0.7 mg AA per mg DEFP resulted in smaller increments in delignification, with values of 84.7 wt% and 84.9 wt%, respectively. Extending the duration of the experiment with a loading of 0.7 mg AA per mg DEFP to 7 h, while keeping all other parameters constant, resulted in a reasonable increase in delignification to 86.4 wt%. Adding AA had a negligible effect on pulp yield as the value decreased from 34.4 wt% (no AA) to 34.1 wt% (0.7 mg AA per mg DEFP) after 4 h. However, increasing the reaction time to 7 h promoted a small decrease in pulp yield to 32.0 wt%. Fig. 5b shows the monomer selectivity of the RCF under the same conditions provided in Fig. 5a. While addition of AA facilitated an increase in monomer yield, it had a negligible effect on monomer selectivity as under all observed conditions, monomer selectivity was approximately 0.29 g mon. per g delig. Collectively, these observations indicate that AA facilitates extraction of lignin from the wood matrix and does not inhibit production of monomers. Considering the trends in monomer yield, delignification, and pulp yield, 0.6 mg AA per mg DEFP loading is a rational optimum loading.

Fig. 5c provides the effects of water as a co-solvent on monomer yield, pulp yield, and delignification. Water as a co-solvent was evaluated as its nucleophilicity could facilitate solvolytic deconstruction of lignins and its low cost and abundance could potentially enhance process viability. Solvent mixtures consisted of equi-volume portions of DMP and water and experiments were conducted at 200 °C using a catalyst dosage of 10 wt% and reaction times of 4 h and 7 h. Overall, addition of water as a co-solvent noticeably improved delignification, but suppressed aromatic monomer yield. For instance, RCF consisting of DMP/H_2O (1 : 1 v/v) observed delignification and monomer yield of 89.2 wt% and 16.2 wt%, respectively; pure DMP treatments resulted in a delignification and monomer yield of 79.1 wt% and 22.9 wt%, respectively. Aqueous DMP mixtures were also prepared with the AA additive (0.6 mg AA per mg DEFP), and interestingly, a monomer yield and delignification of 23.5 wt% and 90.7 wt%, respectively, were observed. As such, aqueous co-solvent with the addition of organic acid additives can maintain monomer yields observed for neat solvent systems yet improve extraction of lignins from softwoods. Pulp yield as anticipated reduced with the increased delignification impact of using water as a co-solvent. With water as co-solvent, pulp yield was 30.0 wt%. The ability of water to enhance delignification albeit at the expense of monomer yield has been noted in some previous studies.[22,85–87] Sels and colleagues evaluated solvent effects in the RCF process and observed that water facilitated the highest delignification, while apolar solvents were less effective.[87] The authors reported that ethylene glycol and MeOH facilitated high delignification, while tetrahydrofuran and 1,4-dioxane (*i.e.*, cyclic ethers) were less efficient for extracting lignins. Nonpolar solvents (*e.g.*, *n*-hexane) were unable to appreciably extract lignin. Furthermore, these studies suggest that increases in lignin extraction and suppression of aromatic monomers may be attributed to competitive adsorption of water to catalytic surface sites, as well as catalyst deactivation facilitated by water-induced leaching of transition metals.[22,85–87]

Mass-based green chemistry benchmarking

The process sustainability of RCF using GDEs was quantitively evaluated using mass-based green chemistry metrics and benchmarking the present study against optimum results reported by previous H_2-free RCF studies; optimum results were considered conditions that facilitated the highest lignin monomer yields within a respective study. Process sustainability was evaluated using mass-based green chemistry metrics, specifically, solvent intensity (SI) and process mass intensity (PMI) as shown by eqn (5) and (6),[88] respectively:

$$\text{Solvent Intensity(SI)} = \frac{\text{mass of solvent}}{\text{mass of product}} \quad (5)$$

$$\text{Process Mass Intensity(PMI)} = \frac{\text{total mass in process(including } H_2O\text{)}}{\text{mass of product}} \quad (6)$$

For both metrics, the total mass of aromatic monomers was considered the mass of the product, with all related masses (*e.g.*, solvents, biomass, catalysts, and additives) confined to the H_2-free RCF process; mass contributions from the biomass

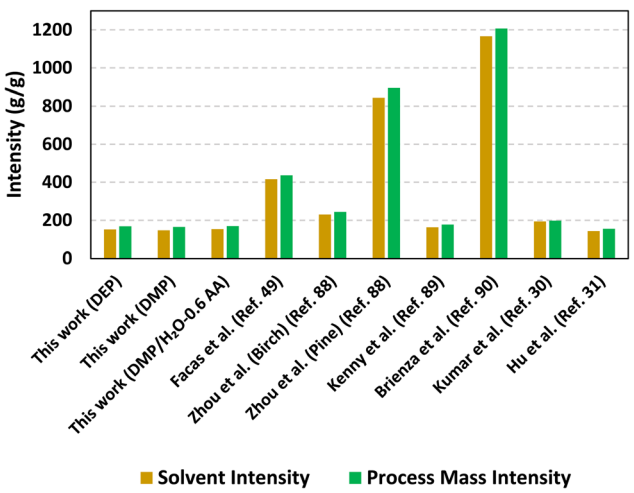

Fig. 6 Comparison of solvent intensity and process mass intensity in the present study and previous H_2-free RCF studies.

Table 1 Mass of reactants and products used for the SI and PMI calculations in the present study and state-of-the-art comparisons

	Biomass (g)	Biomass type	Solvent (g)	Catalyst (g)	Aromatic monomers [product] (g)	SI (g solvent per g monomer)	PMI (g inputs per g monomer)
This work (DEP)	0.73	Softwood	7.31	0.073	0.048	151.5	168.2
This work (DMP)	0.73	Softwood	6.63	0.073	0.045	147.0	164.8
This work (DMP/H_2O-0.6 AA)	0.73	Softwood	7.59	0.073	0.050	153.0	169.1
Facas *et al.* (ref. 49)	1.00	Hardwood	22.20	0.100	0.054	415.3	435.9
Zhou *et al.* (Birch) (ref. 89)	0.50	Hardwood	10.00	0.100	0.043	230.2	244.0
Zhou *et al.* (Pine) (ref. 89)	0.50	Softwood	10.00	0.100	0.012	843.9	894.5
Kenny *et al.* (ref. 90)	2.00	Hardwood	23.73	0.100	0.146	162.7	177.1
Brienza *et al.* (ref. 91)	3.00	Agricultural residue	94.68	0.300	0.081	1166.1	1206.8
Midhun Kumar *et al.* (ref. 30)	0.25	Alkali lignin from pine	15.70	0.050	0.081	193.8	197.5
Hu *et al.* (ref. 31)	2.00	Hardwood	25.70	0.150	0.180	142.7	154.7

pretreatment and downstream separation and isolation steps were not considered. With regard to interpreting the intensity results, lower SI and PMI values indicate more sustainable RCF systems as fewer materials are needed to yield a unit mass of lignin monomers (*i.e.*, products). Fig. 6 provides calculated SI and PMI values for our 5% Pt/C catalyzed experiments performed with DEP, DMP, and DMP in combination with an aqueous co-solvent (1 : 1 v/v) and an organic acid additive (0.6 g AA per g DEFP) under the conditions of 200 °C, 7 h, and 0.1 g cat. per g DEFP, along with optimum results of other studies reported in the literature. In comparison to the state of the art, the SI and PMI values of the present study ranged between 147 and 153 g solvent per g product and ~165 and 169 g inputs per g product, respectively. These values are amongst the lowest reported in the literature, and only the aq. isopropanol-based RCF process of Hu *et al.*[31] facilitated lower SI (142.7 g solvent per g product) and PMI (154.7 g input per g product) values. Higher values of SI and PMI range from ~400 to ~1200 g input per g solvent. Generally, SI and PMI values are similar, indicating the relatively large material footprint solvents have in RCF processes. As such, design of recyclable and benign solvent systems is paramount towards advancing sustainable, lignin-first biorefineries. Table 1 summarizes the quantities of biomass, solvent, and catalyst used, along with the monomer yields associated with the SI and PMI calculations. It is evident that softwood RCF generally achieves lower monomer yield compared to RCF with hardwood and agricultural residues, primarily due to the lower content of cleavable β-O-4 bonds in softwoods.[6,89] Achieving ~0.05 g of aromatic monomers from RCF of pine in the present study, in comparison to the 0.01 g of aromatic monomers reported for RCF of softwood by Zhou *et al.*,[88] is noteworthy and places our results closer to the monomer mass range of 0.04–0.18 g observed in the presented RCF studies with hardwoods and agricultural residues. Overall, the mass-based green chemistry metrics demonstrate that GDEs facilitate materially efficient deconstruction of softwood biomass into value-added aromatic monomers.

MALDI-TOF MS of lignin oils

MALDI-TOF mass spectra of select lignin oil (LO) samples produced *via* H_2-free RCF are shown in Fig. 7. LO consisted of extracted and deconstructed lignins, including monomers and oligomers. Molecular weight ranges of chemical species were categorized as monomers (<250 *m*/*z*), dimers (275–450 *m*/*z*), trimers (450–600 *m*/*z*), tetramers (600–840 *m*/*z*), pentamers (850–1000 *m*/*z*), hexamers (1020–1180 *m*/*z*), and heptamers (1200–1350 *m*/*z*).[92,93] LO samples associated with higher monomer yields had relatively lower molecular weight distribution. For instance, LO produced at 160 °C, 4 h, with 10 wt% catalyst loading, had a monomer yield of 16.1 wt% and molecular weight distribution ranging from 83 *m*/*z* to 1300 *m*/*z*, while LO produced at 200 °C, 7 h, with 10 wt% catalyst loading had a monomer yield of 22.91 wt% and molecular weight distribution ranging from 83 *m*/*z* to 955 *m*/*z*. This trend is reasonable as it simply indicates further deconstruction of oligomeric fragments into monomers under process conditions that enhanced monomer yields. With regard to identification of specific molecular species, mass spectra of 181–182 *m*/*z* likely correspond to hydrogenated forms of coniferyl alcohol, guaiacyl acetone, or hydrogenated variants of hydroxy eugenol. Additionally, spectral peaks at 207–209 *m*/*z* are attributed to dimethoxycinnamic acid and hydrogenated analogs.[93] Within the molecular mass range of dimeric products, significant species may represent various structures such as biphenyl, phenylcoumaran, diarylpropane, and resinol types.[92–94]

Additionally, MALDI-TOF MS facilitated insights into chemical modification of higher molecular weight species. For instance, MALDI TOF mass spectra indicate occurrence of dehydration reactions during H_2-free RCF as several major peaks differentiated by ~18 *m*/*z* (assuming $z = 1$). For example, in Fig. 7b, dehydration is indicated by the following pairs of mass spectra: 83.0–100.8 *m*/*z*, 100.8–118.8 *m*/*z*, 266.2–284.0 *m*/*z*, and 601.2–619.2 *m*/*z*. In addition, decarbonylation reactions evidenced differences of 28 *m*/*z* between the following mass spectral pairs: 434.1–462.1 *m*/*z* and 475.1–503.0 *m*/*z*. Occurrence of dehydration and decarbonylation reactions during RCF was also observed by Medlin and colleagues.[90] These authors conducted RCF using coniferyl alcohol as a model compound and observed that Pd/C and Pt/C catalysts were selective towards formation of 4-ethylguaiacol in comparison to Ru/C and Ni/C. Furthermore, the authors proposed dehydration and decarbonylation pathways as the main pathways towards 4-ethylguaiacol with Pd/C and Pt/C catalysts, while Ru/C and Ni/C primarily performed the hydrodeoxygenation (HDO) reaction.

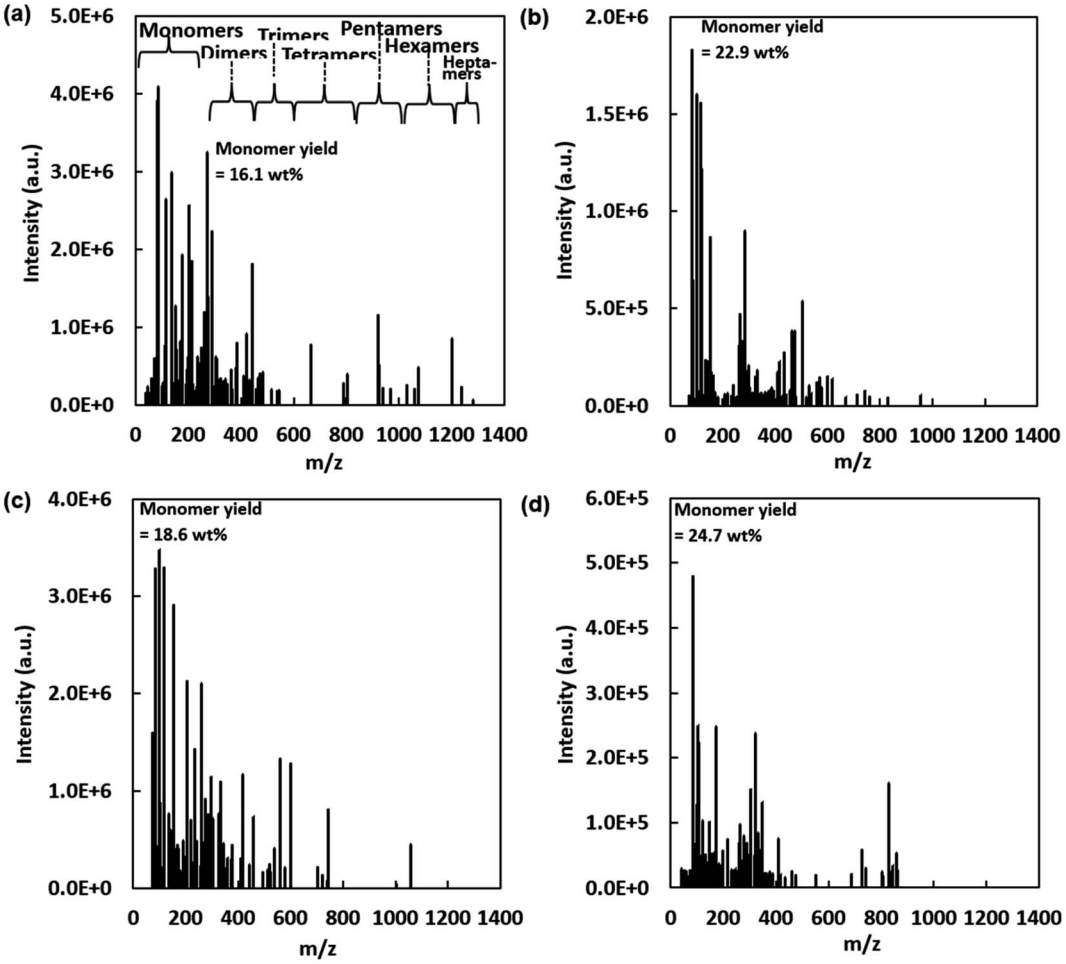

Fig. 7 MALDI-TOF spectra of LOs produced *via* RCF under conditions including (a) DMP, Pt/C, 160 °C, 4 h, (b) DMP, Pt/C, 200 °C, 7 h, (c) DMP, Ru/C, 200 °C, 7 h and (d) DMP/H_2O-0.6 mg AA per mg DEFP, Pt/C, 200 °C, 4 h. Mixing speed and solvent-to-DEFP were 1000 rpm and 0.0096 mL mg^{-1} for (a–d).

NMR characterization of lignin oil

Fig. 8a presents ^1H–^{13}C HSQC NMR spectra of LO produced from H_2-free RCF conducted at 200 °C for 7 h, using DMP as solvent and 10 wt% catalyst dosage. Cross-peaks were assigned using previous reports in the literature.[23,95,96] β-O-4 linkages, the most abundant native linkage, were absent. Furthermore, all ^1H–^{13}C HSQC NMR spectra were absent of native β-5 phenylcoumaran units. Instead, spectra indicated the presence of β-5 propanol (β-5 γ-OH) and β-5 ethyl (β-5 (E)) derivatives, which are obtained through hydrogenolysis of the etheric ring and hydrodeoxygenation, respectively. Similarly, native β–β resinol, β-1 spirodieneone, and 5–5 dibenzodioxicin structures were not present in the LO. Instead, hydrogenated forms of β–β THF, β-1 propanol (β-1 γ-OH), and 5–5 biphenyl were observed.

Neat solvolysis experiments were conducted in the absence of the catalyst to facilitate insights into the role of competing reaction processes (*e.g.*, solvolysis and hydrogenolysis) on the deconstruction of lignins. Fig. 8b provides ^1H–^{13}C HSQC NMR spectra of LO produced *via* neat solvolysis under the same conditions as those in Fig. 8a. Interestingly, a weak β-O-4 cross peak was observed in the 2D HSQC NMR spectrum of LO produced by neat solvolysis. Furthermore, cross peaks indicative of other native structures, including β-5 phenylcoumaran and β–β resinol, were present in the ^1H–^{13}C HSQC NMR spectra. However, the signals corresponding to these native units were relatively weak compared to the signals of their hydrogenated forms, which were also present in the spectrum. The presence of β-O-4 linkages in solvolytic lignins indicates that hydrogenolysis pathways enabled by transition metal catalysts contribute to the lysing of etheric linkages. Furthermore, the presence of native C–C linkages in the solvolytic lignins indicates that reductive pathways contribute towards their deconstruction and/or chemical modification. Previous reports have indicated that transition metal catalysts facilitate reductive stabilization of reactive intermediates.[49,74,97,98] For reference, Fig. S2 and S3† provide ^1H NMR spectra for H_2-free RCF and neat solvolysis.

Furan derivative yield

In addition to aromatic monomers, other value-added small molecules, including furans derived from holocellulose, can be

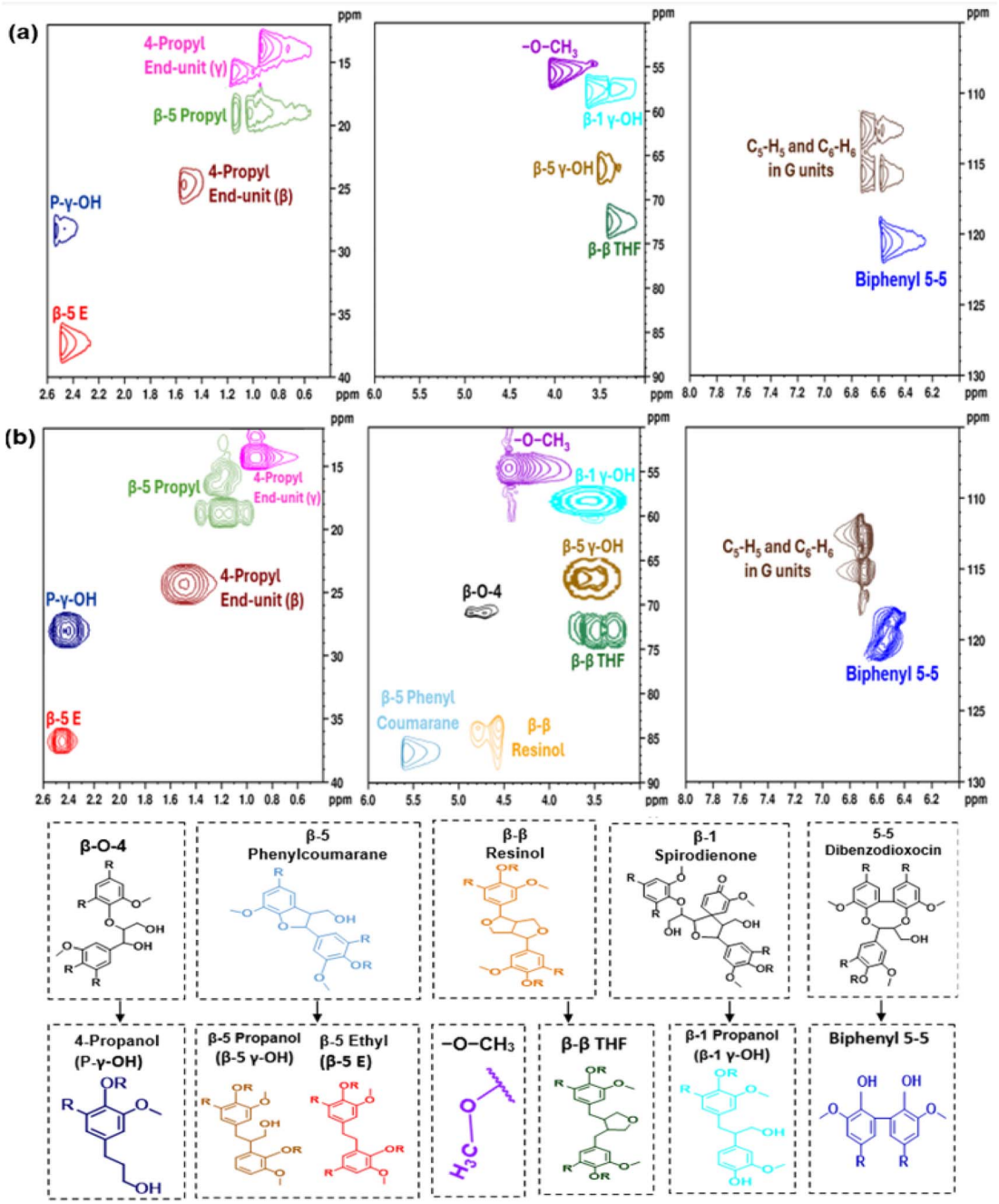

Fig. 8 (a) $^{1}H-^{13}C$ HSQC NMR spectra of LO resulting from H_2-free RCF using 10 wt% Pt/C loading. (b) $^{1}H-^{13}C$ HSQC NMR spectra of LO resulting from neat solvolysis. Reaction conditions: 730 mg DEFP, 7 mL DMP, 200 °C, 7 h, 0.0096 mL per mg solvent-to-DEFP ratio, 1000 rpm.

produced during solvolysis and hydrogenolysis of lignocellulosic biomass. Fig. 9 provides yields of furan derivatives resulting from neat solvolysis and H_2-free RCF of lodgepole pine conducted at 200 °C and 7 h using DMP; the offered yields are normalized by the holocellulose content of lodgepole line. Previously, furans have been reported as minor products resulting from catalytic fractionation.[99–101] Similar furan species were yielded from both neat solvolysis and RCF, including 2-furaldehyde, 5-hydroxymethylfurfural (5-HMF), furan-2,5-dicarboxylic acid, and tetrahydrofuran. Levulinic acid was also produced, which is derived from ring opening of 5-HMF. Based on an initial holocellulose content of 71.1% (519.0 mg of holocellulose in 730 mg DEFP), neat solvolysis, Ru/C catalyzed RCF, and Pt/C catalyzed RCF facilitated total furan yields of 8.1 wt%, 4.7 wt%, and 4.2 wt%, respectively. Interestingly, the presence of supported transition metal catalysts induced lower yields of furans, which could be due to hydrogenation and hydrogenolysis of the observed furanic species. Fig. S4† shows that on a DEFP mass basis, neat solvolysis results in a higher yield of furan derivatives compared to monomers, while H_2-free RCF favors the opposite trend. While reduced forms

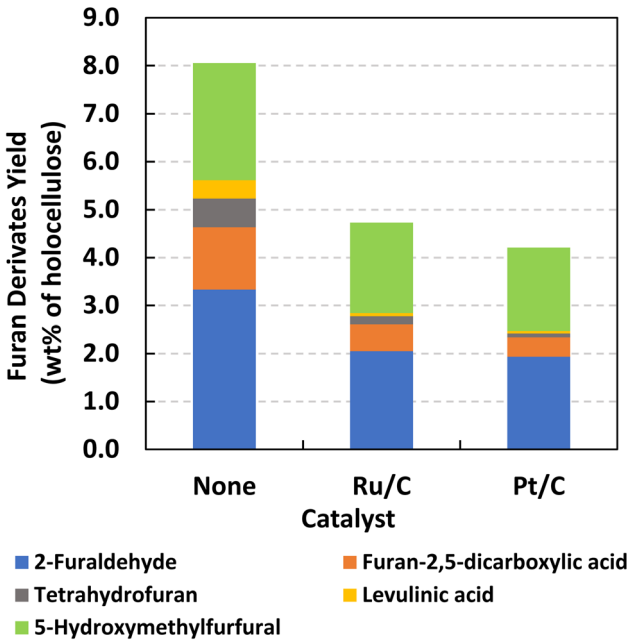

Fig. 9 Yields of furan derivatives from neat solvolysis and H_2-free RCF. Reaction conditions: 730 mg DEFP, 7 mL DMP, 73 mg catalyst, 200 °C, 7 h, 0.1 g per g catalyst dosage, 0.0096 mL per mg solvent-to-DEFP ratio, 1000 RPM.

of the observed furanic species were not directly detected in the present study, there is potential for GDEs to facilitate valorization of furans *via* transfer hydrogenolysis pathways in future studies.

Influence of H_2-free RCF on cellulosic pulps

RCF studies focus primarily on depolymerization of lignins; however, residual cellulosic pulps constitute a major product fraction (~30 to 40 wt%) that will contribute to the economic viability of biorefining paradigms. Hence, crystallographic and morphological characteristics of residual pulps resulting from H_2-free RCF are provided in Fig. 10. Fig. 10a provides XRD diffractograms of DEFP and residual pulps from select experiments. XRD indicated DEFP and residual pulps displayed diffractogram patterns characteristic of cellulose I_β, specifically peaks observed at 2θ of 16.3°, 22.5°, and 34.7°.[102] Residual pulps displayed lower XRD signal intensities than DEFP, with the crystallinity index [CI (%)] following a decreasing order: DEFP – blue (52.1%) > pulp produced from DMP RCF conducted at 160 °C, 4 h, 10 wt% Pt/C catalyst dosage yellow – (36.3%) > pulp produced from DEP RCF conducted at 200 °C, 7 h, 10 wt% Pt/C catalyst dosage – red (35.8%) > pulp produced from DMP RCF conducted at 200 °C, 7 h, 10 wt% Pt/C catalyst dosage – green (31.4%). CI was calculated in accordance with Segal's method,[103] with the relevant equations and calculations provided in Section A of the ESI.† Reduced crystallinity of the resultant pulps can be due to chemical deconstruction of crystalline domains within the native cellulosic matrix; reduction in crystallinity of pulps with a negligible change in diffractogram patterns has been previously reported.[104,105] Fig. 10 (b–e) provide SEM micrographs of the same DEFP and residual pulp samples provided in Fig. 10a. Overall, the shape, texture, and surface structure of lignocellulosic pulps are analogous to those of raw wood.

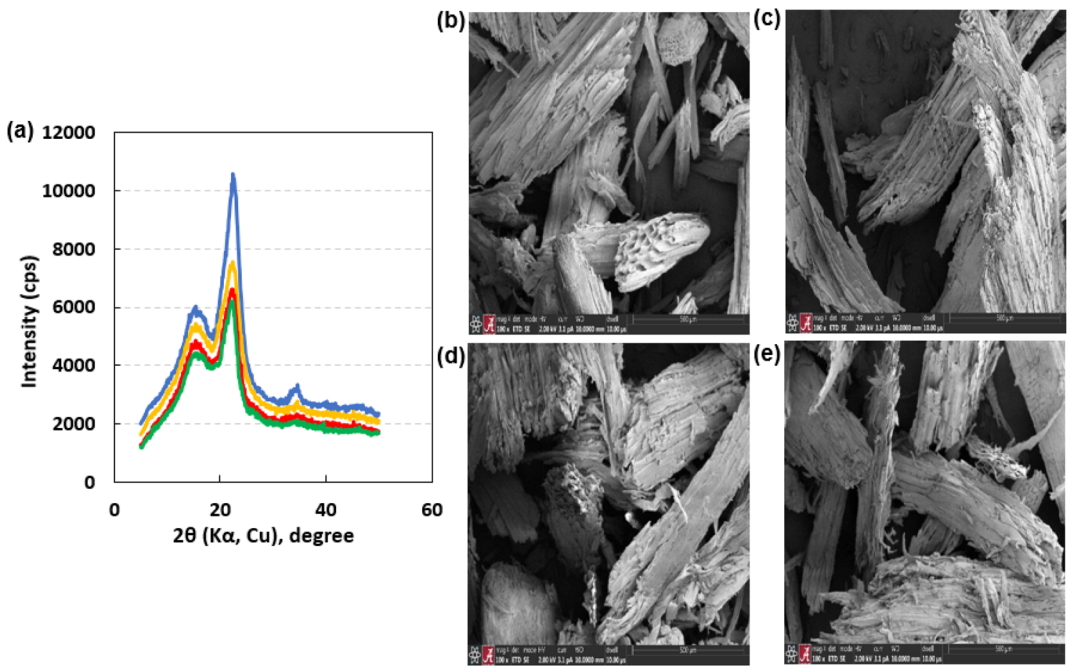

Fig. 10 (a) XRD of DEFP (blue), pulp produced from DMP RCF conducted at 160 °C, 4 h, 10 wt% Pt/C catalyst dosage (yellow), pulp produced from DEP RCF conducted at 200 °C, 7 h, 10 wt% Pt/C catalyst dosage (red), and pulp produced from DMP RCF conducted at 200 °C, 7 h, 10 wt% Pt/C catalyst dosage (green); SEM micrographs of DEFP (b) and residual pulps corresponding to the XRD samples ((c) – yellow, (d) – red, and (e) – green).

Conclusion

GDEs have been demonstrated as effective hydrogen transfer solvents for supporting lignin deconstruction into functionalized monomers under mild conditions. Monomer yields of ~20 wt% to ~25 wt% were achieved and delignification approaching ~90 wt% was achieved in the presence of aqueous and organic acid additives; these values are competitive with previous reports for softwoods. Monomer yields are improved in the presence of organic acid additives and are reduced when RCF is conducted in aqueous co-solvent (without organic acid). Both AA additives and aqueous co-solvent facilitated enhanced delignification of lodgepole pine. Aromatic monomers consisted primarily of species with unsaturated and oxygenated sidechains, including vanillin, *trans*-isoeugenol, coniferaldehyde, eugenol, and vanillic acid. Production of functionalized aromatics, especially those rich in oxygenated functionalities, contrasts with prior RCF reports which primarily observed monomers with saturated alkyl sidechains (*e.g.*, 4-propylguaiacol, 4-ethylguaiacol). This observation demonstrates that GDEs can support valorization of lignocellulosic biomass directly to value-added species suitable for fragrances and flavorants (*e.g.*, vanillin, coniferaldehyde). Other small molecule product streams included furanic monomers derived from carbohydrate fractions, with higher yields observed for neat solvolysis than for RCF, as the latter likely facilitated their reduction. Mass-based green chemistry metrics demonstrated that GDEs facilitate materially efficient RCF of softwood biomass into value-added monomers. MALDI-TOF MS of lignin oils indicated that the sidechains of higher molecular weight species undergo dehydration and decarbonylation reactions. ^{1}H–^{13}C HSQC NMR demonstrated the presence of native linkages in lignin oils produced by neat solvolysis whereas samples resulting from H_2-free RCF lacked native linkages, thus indicating the role of catalysts in facilitating hydrogenolysis. Residual pulps resulting from H_2-free RCF were produced at yields of ~30 to 40 wt% and maintained crystalline structures and overall morphology of the softwood feedstock. Collectively, these findings demonstrate the efficacy of GDEs for H_2-free RCF of softwood biomass into valuable aromatic and furanic monomers, which can be leveraged towards the development of sustainable and environmentally cogent lignin valorization processes. Future studies should consider roles of catalyst supports on transfer hydrogenolysis pathways facilitating deconstruction of recalcitrant oligomers in order to improve production of value-added aromatic monomers.

Data availability

All required data for evaluating the conclusions are provided in the paper and ESI.† Additional data can be obtained from the authors upon request.

Author contributions

Bernard C. Ekeoma: investigation, validation, data curation, writing – original draft. Jason E. Bara: resources, methodology, writing – review & editing. James D. Sheehan: conceptualization, methodology, validation, data curation, resources, writing – original draft, writing – review & editing, visualization, supervision, project administration, funding acquisition.

Conflicts of interest

The authors declare that they have no known competing financial interests or personal relationships that could have appeared to influence the work reported in this paper.

Acknowledgements

This work was partially supported by the University of Alabama Office for Research and Economic Development Small Grants Program (Award # RG14968) and Agricultural and Food Research Initiative grant no. 2023-67022-39593 from the USDA National Institute of Food and Agriculture. The authors thank the Idaho National Lab Bioenergy Feedstock Library for supplying the samples of lodgepole pine.

References

1 U.S. Energy Information Administration (EIA), EIA projects nearly 50% increase in world energy usage by 2050, led by growth in Asia, https://www.eia.gov/todayinenergy/detail.php?id=41433.
2 G. E. Halkos and E. C. Gkampoura, Reviewing Usage, Potentials, and Limitations of Renewable Energy Sources, *Energies*, 2020, **13**(11), 2906–2925, DOI: 10.3390/EN13112906.
3 G. Lopez, D. Keiner, M. Fasihi, T. Koiranen and C. Breyer, From Fossil to Green Chemicals: Sustainable Pathways and New Carbon Feedstocks for the Global Chemical Industry, *Energy Environ. Sci.*, 2023, **16**(7), 2879–2909, DOI: 10.1039/D3EE00478C.
4 W. Deng, Y. Feng, J. Fu, H. Guo, Y. Guo, B. Han, Z. Jiang, L. Kong, C. Li, H. Liu, P. T. T. Nguyen, P. Ren, F. Wang, S. Wang, Y. Wang, Y. Wang, S. S. Wong, K. Yan, N. Yan, X. Yang, Y. Zhang, Z. Zhang, X. Zeng and H. Zhou, Catalytic Conversion of Lignocellulosic Biomass into Chemicals and Fuels, *Green Energy Environ.*, 2023, **8**(1), 10–114, DOI: 10.1016/J.GEE.2022.07.003.
5 P. Joshi, R. Roy, S. Rahman, T. A. Amit and B. Jadhav, Recent Advances in Lignin Depolymerization Techniques: A Comparative Overview of Traditional and Greener Approaches, *Biomass*, 2022, **2**(3), 130–154, DOI: 10.3390/BIOMASS2030009.
6 W. Schutyser, T. Renders, S. Van Den Bosch, S. F. Koelewijn, G. T. Beckham and B. F. Sels, Chemicals from Lignin: An Interplay of Lignocellulose Fractionation, Depolymerisation, and Upgrading, *Chem. Soc. Rev.*, 2018, **47**(3), 852–908, DOI: 10.1039/C7CS00566K.
7 M. Mujtaba, L. Fernandes Fraceto, M. Fazeli, S. Mukherjee, S. M. Savassa, G. Araujo de Medeiros, A. do Espírito Santo Pereira, S. D. Mancini, J. Lipponen and F. Vilaplana, Lignocellulosic Biomass from Agricultural Waste to the

Circular Economy: A Review with Focus on Biofuels, Biocomposites and Bioplastics, *J. Cleaner Prod.*, 2023, **402**, 136815, DOI: 10.1016/J.JCLEPRO.2023.136815.

8 F. H. Isikgor and C. R. Becer, Lignocellulosic Biomass: A Sustainable Platform for the Production of Bio-Based Chemicals and Polymers, *Polym. Chem.*, 2015, **6**(25), 4497–4559, DOI: 10.1039/C5PY00263J.

9 L. Petridis and J. C. Smith, Molecular-Level Driving Forces in Lignocellulosic Biomass Deconstruction for Bioenergy, *Nat. Rev. Chem*, 2018, **2**(11), 382–389, DOI: 10.1038/s41570-018-0050-6.

10 B. Singh, J. Korstad, A. Guldhe and R. Kothari, Editorial: Emerging Feedstocks & Clean Technologies for Lignocellulosic Biofuel, *Front. Energy Res.*, 2022, **10**, 917081, DOI: 10.3389/FENRG.2022.917081/BIBTEX.

11 BETO: Billion-Ton 2023 | Department of Energy, https://www.energy.gov/eere/bioenergy/2023-billion-ton-report-assessment-us-renewable-carbon-resources, accessed 2024-04-25.

12 S. N. Oswalt, W. B. Smith, P. D. Miles and S. A. Pugh, *Forest Resources of the United States, 2017 A Technical Document Supporting the Forest Service 2020 RPA Assessment*. 2017, DOI: 10.2737/WO-GTR-97.

13 J. Han, C. E. Canter, H. Cai, M. Wang, Z. Qin, J. B. Dunn, R. Gustafson, S. S. Kelley; R. Morales, E. E. Oneil, L. OU, S. Park, M. Puettmann, N. Rajagopalan, T. A. Volk and A. Weiskittel, *Carbon Dynamics for Biofuels Produced from Woody Feedstocks*, ANL, 2018, DOI: 10.13140/RG.2.2.21103.79526.

14 L. Li, L. Dong, D. Li, Y. Guo, X. Liu and Y. Wang, Hydrogen-Free Production of 4-Alkylphenols from Lignin via Self-Reforming-Driven Depolymerization and Hydrogenolysis, *ACS Catal.*, 2020, **10**(24), 15197–15206, DOI: 10.1021/acscatal.0c03170.

15 M. J. Gan, Y. Q. Niu, X. J. Qu and C. H. Zhou, Lignin to Value-Added Chemicals and Advanced Materials: Extraction, Degradation, and Functionalization, *Green Chem.*, 2022, **24**(20), 7705–7750, DOI: 10.1039/D2GC00092J.

16 Y. Zhan, M. Wang, T. Ma and Z. Li, Enhancing the Potential Production of Bioethanol with Bamboo by γ-Valerolactone/Water Pretreatment, *RSC Adv.*, 2022, **12**(26), 16942–16954, DOI: 10.1039/D2RA02421G.

17 S. Beluhan, K. Mihajlovski, B. Šantek and M. Ivanči, The Production of Bioethanol from Lignocellulosic Biomass: Pretreatment Methods, Fermentation, and Downstream Processing, *Energies*, 2023, **16**(19), 7003–7041, DOI: 10.3390/EN16197003.

18 A. Beaucamp, M. Muddasar, I. S. Amiinu, M. Moraes Leite, M. Culebras, K. Latha, M. C. Gutiérrez, D. Rodriguez-Padron, F. del Monte, T. Kennedy, K. M. Ryan, R. Luque, M. M. Titirici and M. N. Collins, Lignin for Energy Applications – State of the Art, Life Cycle, Technoeconomic Analysis and Future Trends, *Green Chem.*, 2022, **24**(21), 8193–8226, DOI: 10.1039/D2GC02724K.

19 C. Vasile, M. Baican, R. Academy and P. Poni, Lignins as Promising Renewable Biopolymers and Bioactive Compounds for High-Performance Materials, *Polymers*, 2023, **15**(15), 3177, DOI: 10.3390/POLYM15153177.

20 J. D. Sheehan, E. Ebikade, D. G. Vlachos and R. F. Lobo, Lignin-Based Water-Soluble Polymers Exhibiting Biodegradability and Activity as Flocculating Agents, *ACS Sustainable Chem. Eng.*, 2022, **10**(34), 11117–11129, DOI: 10.1021/acssuschemeng.2c01428.

21 J. H. Jang, D. G. Brandner, R. J. Dreiling, A. J. Ringsby, J. R. Bussard, L. M. Stanley, R. M. Happs, A. S. Kovvali, J. I. Cutler, T. Renders, J. R. Bielenberg, Y. Román-Leshkov and G. T. Beckham, Multi-Pass Flow-through Reductive Catalytic Fractionation, *Joule*, 2022, **6**(8), 1859–1875, DOI: 10.1016/J.JOULE.2022.06.016.

22 J. H. Jang, A. R. C. Morais, M. Browning, D. G. Brandner, J. K. Kenny, L. M. Stanley, R. M. Happs, A. S. Kovvali, J. I. Cutler, Y. Román-Leshkov, J. R. Bielenberg and G. T. Beckham, Feedstock-Agnostic Reductive Catalytic Fractionation in Alcohol and Alcohol–Water Mixtures, *Green Chem.*, 2023, **25**(9), 3660–3670, DOI: 10.1039/D2GC04464A.

23 K. Van Aelst, E. Van Sinay, T. Vangeel, E. Cooreman, G. Van Den Bossche, T. Renders, J. Van Aelst, S. Van Den Bosch and B. F. Sels, Reductive Catalytic Fractionation of Pine Wood: Elucidating and Quantifying the Molecular Structures in the Lignin Oil, *Chem. Sci.*, 2020, **11**(42), 11498–11508, DOI: 10.1039/D0SC04182C.

24 T. Ren, S. You, Z. Zhang, Y. Wang, W. Qi, R. Su and Z. He, Highly Selective Reductive Catalytic Fractionation at Atmospheric Pressure without Hydrogen, *Green Chem.*, 2021, **23**(4), 1648–1657, DOI: 10.1039/D0GC03314F.

25 T. Renders, W. Schutyser, S. Van Den Bosch, S. F. Koelewijn, T. Vangeel, C. M. Courtin and B. F. Sels, Influence of Acidic (H3PO4) and Alkaline (NaOH) Additives on the Catalytic Reductive Fractionation of Lignocellulose, *ACS Catal.*, 2016, **6**(3), 2055–2066, DOI: 10.1021/acscatal.5b02906.

26 O. P. Taran, A. V. Miroshnikova, S. V. Baryshnikov, A. S. Kazachenko, A. M. Skripnikov, V. V. Sychev, Y. N. Malyar and B. N. Kuznetsov, Reductive Catalytic Fractionation of Spruce Wood over Ru/C Bifunctional Catalyst in the Medium of Ethanol and Molecular Hydrogen, *Catalysts*, 2022, **12**(11), 1384–1406, DOI: 10.3390/CATAL12111384.

27 E. O. Ebikade, N. Samulewicz, S. Xuan, J. D. Sheehan, C. Wu and D. G. Vlachos, Reductive Catalytic Fractionation of Agricultural Residue and Energy Crop Lignin and Application of Lignin Oil in Antimicrobials, *Green Chem.*, 2020, **22**(21), 7435–7447, DOI: 10.1039/d0gc02781b.

28 X. Mei, H. Liu, H. Wu, W. Wu, B. Zheng, Y. Liu, X. Zheng, Y. Wang, W. Han and B. Han, Catalytic Self-Transfer Hydrogenolysis of Lignin over Ni/C Catalysts, *Green Chem.*, 2024, **26**(8), 4544–4551, DOI: 10.1039/D3GC04217K.

29 X. Lu, H. Guo, J. Chen, D. Wang, A. F. Lee and X. Gu, Selective Catalytic Transfer Hydrogenation of Lignin to Alkyl Guaiacols Over NiMo/Al-MCM-41, *ChemSusChem*, 2022, **15**(7), e202200099, DOI: 10.1002/CSSC.202200099.

30 M. Midhun Kumar, L. Gurrala, C. Paek and R. Vinu, Selective Production of Guaiacol from Lignin via Catalytic

Transfer Hydrogenolysis Using Ru-Cu/Zirconia, *Mol. Catal.*, 2022, **530**, 112532, DOI: 10.1016/J.MCAT.2022.112532.

31 J. Hu, M. Zhao, B. Jiang, S. Wu and P. Lu, Catalytic Transfer Hydrogenolysis of Native Lignin to Monomeric Phenols over a Ni-Pd Bimetallic Catalyst, *Energy Fuel.*, 2020, **34**(8), 9754–9762, DOI: 10.1021/acs.energyfuels.0c01962.

32 J. A. Godwin, J. P. Babusci, N. M. Wonderling, J. R. Shallenberger, K. Seabright, D. P. Harper and S. C. Chmely, Catalytic Transfer Hydrogenolysis of Switchgrass Lignin with Ethanol Using Spinel-Type Mixed-Metal Oxide Catalysts Affords Control of the Oxidation State of Isolated Aromatic Products, *ACS Sustainable Chem. Eng.*, 2024, **12**(7), 2611–2620, DOI: 10.1021/acssuschemeng.3c06392.

33 M. M. Kumar, V. S. Prabhudesai and R. Vinu, Lignin Depolymerization to Guaiacol and Vanillin Derivatives via Catalytic Transfer Hydrogenolysis Using Pd-Lewis Metal Oxide Supported on Activated Carbon Catalysts, *Mol. Catal.*, 2023, **549**, 113474, DOI: 10.1016/J.MCAT.2023.113474.

34 Y. Li, M. Liu, Q. Tang, K. Liang, Y. Sun, Y. Yu, Y. Lou and Y. Liu, Hydrogen-transfer strategy in lignin refinery: Towards sustainable and versatile value-added biochemicals, *ChemSusChem*, 2024, **17**(12), e202301912, DOI: 10.1002/cssc.202301912.

35 Y. Li, Y. Yu, Y. Lou, S. Zeng, Y. Sun, Y. Liu and H. Yu, Hydrogen-Transfer Reductive Catalytic Fractionation of Lignocellulose: High Monomeric Yield with Switchable Selectivity, *Angew. Chem., Int. Ed.*, 2023, **62**(32), e202307116, DOI: 10.1002/anie.202307116.

36 F. Valentini, A. Marrocchi and L. Vaccaro, Liquid Organic Hydrogen Carriers (LOHCs) as H-Source for Bio-Derived Fuels and Additives Production, *Adv. Energy Mater.*, 2022, **12**(13), 2103362, DOI: 10.1002/AENM.202103362.

37 Y. Ni, Z. Han, Y. Chai, G. Wu and L. Landong, Catalytic Hydrogen Storage in Liquid Hydrogen Carriers, *EES Catal.*, 2023, **1**(4), 459–494, DOI: 10.1039/D3EY00076A.

38 F. Ferlin, F. Valentini, A. Marrocchi and L. Vaccaro, Catalytic Biomass Upgrading Exploiting Liquid Organic Hydrogen Carriers (LOHCs), *ACS Sustainable Chem. Eng.*, 2021, **9**(29), 9604–9624, DOI: 10.1021/acssuschemeng.1c03247.

39 X. Shen, C. Zhang, B. Han and F. Wang, Catalytic Self-Transfer Hydrogenolysis of Lignin with Endogenous Hydrogen: Road to the Carbon-Neutral Future, *Chem. Soc. Rev.*, 2022, **51**(5), 1608–1628, DOI: 10.1039/D1CS00908G.

40 X. Du, S. Wu and P. Li, Catalytic Hydrogenolysis Lignin to Obtain Phenols: A Review of Selective Cleavage of Ether Bonds, *Bioresources*, 2023, **18**(2), 4231–4261, DOI: 10.15376/BIORES.18.2.DU.

41 J. Zhang, Catalytic Transfer Hydrogenolysis as an Efficient Route in Cleavage of Lignin and Model Compounds, *Green Energy Environ.*, 2018, **3**(4), 328–334, DOI: 10.1016/J.GEE.2018.08.001.

42 X. Mei, H. Liu, H. Wu, W. Wu, B. Zheng, Y. Liu, X. Zheng, Y. Wang, W. Han and B. Han, Catalytic Self-Transfer Hydrogenolysis of Lignin over Ni/C Catalysts, *Green Chem.*, 2024, **26**(8), 4544–4551, DOI: 10.1039/D3GC04217K.

43 N. A. B. Aponte and V. Meille, Use of BioSource Molecules as Liquid Organic Hydrogen Carriers (LOHC) and for Circular Storage, *Reactions*, 2024, **5**(1), 195–212, DOI: 10.3390/REACTIONS5010008.

44 C. Chu, K. Wu, B. Luo, Q. Cao and H. Zhang, Hydrogen Storage by Liquid Organic Hydrogen Carriers: Catalyst, Renewable Carrier, and Technology – A Review, *Carbon Resour. Convers.*, 2023, **6**(4), 334–351, DOI: 10.1016/J.CRCON.2023.03.007.

45 G. Fraga, Y. Yin, M. Konarova, M. D. Hasan, B. Laycock, Q. Yuan, N. Batalha and S. Pratt, Hydrocarbon hydrogen carriers for catalytic transfer hydrogenation of guaiacol, *Int. J. Hydrogen Energy*, 2020, **45**(51), 27381–27391, DOI: 10.1016/j.ijhydene.2020.07.136.

46 A. E. Díaz-álvarez and V. Cadierno, Glycerol: A Promising Green Solvent and Reducing Agent for Metal-Catalyzed Transfer Hydrogenation Reactions and Nanoparticles Formation, *Appl. Sci.*, 2013, **3**(1), 55–69, DOI: 10.3390/APP3010055.

47 G. Zhang, J. Zhao, X. Jin, Y. Qian, M. Zhou, X. Jia, F. Sun, J. Jiang, W. Xu and B. Sun, Combined Dehydrogenation of Glycerol with Catalytic Transfer Hydrogenation of H_2 Acceptors to Chemicals: Opportunities and Challenges, *Front. Chem.*, 2022, **10**, 962579, DOI: 10.3389/FCHEM.2022.962579/BIBTEX.

48 R. M. O'Dea, P. A. Pranda, Y. Luo, A. Amitrano, E. O. Ebikade, E. R. Gottlieb, O. Ajao, M. Benali, D. G. Vlachos, M. Ierapetritou and T. H. Epps, Ambient-Pressure Lignin Valorization to High-Performance Polymers by Intensified Reductive Catalytic Deconstruction, *Sci. Adv.*, 2022, **8**(3), 7523, DOI: 10.1126/sciadv.abj7523.

49 G. G. Facas, D. G. Brandner, J. R. Bussard, Y. Román-Leshkov and G. T. Beckham, Interdependence of Solvent and Catalyst Selection on Low Pressure Hydrogen-Free Reductive Catalytic Fractionation, *ACS Sustain. Chem. Eng.*, 2023, **11**(12), 4517–4522, DOI: 10.1021/acssuschemeng.2c07394.

50 D. Prat, A. Wells, J. Hayler, H. Sneddon, C. R. McElroy, S. Abou-Shehada and P. J. Dunn, CHEM21 Selection Guide of Classical- and Less Classical-Solvents, *Green Chem.*, 2015, **18**(1), 288–296, DOI: 10.1039/C5GC01008J.

51 P. T. Anastas and J. C. Warner, Green Chemistry, *Org. Process Res. Dev.*, 2000, **4**(5), 437–438, DOI: 10.1021/OP000054t.

52 J. Fowles, M. Banton, J. Klapacz and H. Shen, A toxicological review of the ethylene glycol series: Commonalities and differences in toxicity and modes of action, *Toxicol. Lett.*, 2017, **278**, 66–83, DOI: 10.1016/j.toxlet.2017.06.009.

53 Q. Yang, Q. Yang, S. Xu, S. Zhu and D. Zhang, Technoeconomic and Environmental Analysis of Ethylene Glycol Production from Coal and Natural Gas Compared with Oil-Based Production, *J. Cleaner Prod.*, 2020, **273**, 123120, DOI: 10.1016/J.JCLEPRO.2020.123120.

54 A. Soyemi and T. Szilvási, Calculated Physicochemical Properties of Glycerol-Derived Solvents to Drive Plastic Waste Recycling, *Ind. Eng. Chem. Res.*, 2023, **62**(15), 6322–6337, DOI: 10.1021/acs.iecr.2c04567.

55 Q. Hou, M. Zhen, H. Qian, Y. Nie, X. Bai, T. Xia, M. Laiq Ur Rehman, Q. Li and M. Ju, Upcycling and Catalytic Degradation of Plastic Wastes, *Cell Rep. Phys. Sci.*, 2021, **2**(8), 100514, DOI: 10.1016/J.XCRP.2021.100514.

56 P. Lomwongsopon and C. Varrone, Critical Review on the Progress of Plastic Bioupcycling Technology as a Potential Solution for Sustainable Plastic Waste Management, *Polymers*, 2022, **14**(22), 4996, DOI: 10.3390/POLYM14224996.

57 S. Qian, X. Liu, G. P. Dennis, C. H. Turner and J. E. Bara, Properties of Symmetric 1,3-Diethers Based on Glycerol Skeletons for CO2 Absorption, *Fluid Phase Equilib.*, 2020, **521**, 112718, DOI: 10.1016/J.FLUID.2020.112718.

58 B. S. Flowers, M. S. Mittenthal, A. H. Jenkins, D. A. Wallace, J. W. Whitley, G. P. Dennis, M. Wang, H. C. Turner, V. N. Emel'yanenko, S. P. Verevkin and J. E. Bara, 1,2,3-Trimethoxypropane: A Glycerol-Derived Physical Solvent for CO2 Absorption, *ACS Sustainable Chem. Eng.*, 2016, **5**(1), 911–921, DOI: 10.1021/acssuschemeng.6b02231.

59 Z. Huang, B. Jiang, H. Yang, B. Wang, N. Zhang, H. Dou, G. Wei, Y. Sun and L. Zhang, Investigation of Glycerol-Derived Binary and Ternary Systems in CO2 Capture Process, *Fuel*, 2017, **210**, 836–843, DOI: 10.1016/J.FUEL.2017.08.043.

60 A. Leal-Duaso, P. Pérez, J. A. Mayoral, J. I. Garciá and E. Pires, Glycerol-Derived Solvents: Synthesis and Properties of Symmetric Glyceryl Diethers, *ACS Sustainable Chem. Eng.*, 2019, **7**(15), 13004–13014, DOI: 10.1021/acssuschemeng.9b02105.

61 K. A. Agwu, S. R. Belmont, J. M. Enguita and J. D. Sheehan, Polar Aprotic Solvent Properties Influence Pulp Characteristics and Delignification Kinetics of CO2/Organic Base Organosolv Pretreatments of Lignocellulosic Biomass, *Chem. Eng. Sci.*, 2024, **288**, 119808, DOI: 10.1016/J.CES.2024.119808.

62 A. Sluiter, R. Ruiz, C. Scarlata, J. Sluiter and D. Templeton, *Determination of Extractives in Biomass*, Laboratory Analytical Procedure (LAP), 2008.

63 A. Sluiter, B. Hames, R. Ruiz, C. Scarlata, J. Sluiter, D. Templeton and D. Crocker, *Determination of Structural Carbohydrates and Lignin in Biomass*, Laboratory Analytical Procedure (LAP). 2008.

64 A. Sluiter, B. Hames, R. Ruiz, C. Scarlata, J. Sluiter and D. Templeton, *Determination of Ash in Biomass*, Laboratory Analytical Procedure (LAP), 2008.

65 X. Liu, H. Li, L. P. Xiao, R. C. Sun and G. Song, Chemodivergent Hydrogenolysis of Eucalyptus Lignin with Ni@ZIF-8 Catalyst, *Green Chem.*, 2019, **21**(6), 1498–1504, DOI: 10.1039/C8GC03511C.

66 J. Rencoret, A. Gutiérrez, L. Nieto, J. Jiménez-Barbero, C. B. Faulds, H. Kim, J. Ralph, Á. T. Martínez and J. C. del Río, Lignin Composition and Structure in Young versus Adult Eucalyptus Globulus Plants, *Plant Physiol.*, 2011, **155**(2), 667–682, DOI: 10.1104/PP.110.167254.

67 A. Margellou and K. S. Triantafyllidis, Catalytic Transfer Hydrogenolysis Reactions for Lignin Valorization to Fuels and Chemicals, *Catalysts*, 2019, **9**(1), 43, DOI: 10.3390/CATAL9010043.

68 Y. N. Regmi, J. K. Mann, J. R. McBride, J. Tao, C. E. Barnes, N. Labbé and S. C. Chmely, Catalytic Transfer Hydrogenolysis of Organosolv Lignin Using B-Containing FeNi Alloyed Catalysts, *Catal. Today*, 2018, **302**, 190–195, DOI: 10.1016/J.CATTOD.2017.05.051.

69 L. Gurrala, M. M. Kumar and R. Vinu, Catalytic Hydrogenolysis of Lignin to Phenols: Effect of Operating Conditions on Product Distribution, *Biomass, Biofuels, Biochemicals: Lignin Biorefinery*, 2021, pp. 83–107, DOI: 10.1016/B978-0-12-820294-4.00001-6.

70 J. A. Sirviö, I. Romakkaniemi, J. Ahola, S. Filonenko, J. P. Heiskanen and A. Ämmälä, Supramolecular Interaction-Driven Delignification of Lignocellulose, *Green Chem.*, 2024, **26**(1), 287–294, DOI: 10.1039/D3GC03857B.

71 R. Rinken, D. Posthuma and R. Rinaldi, Lignin Stabilization and Carbohydrate Nature in H-Transfer Reductive Catalytic Fractionation: The Role of Solvent Fractionation of Lignin Oil in Structural Profiling, *ChemSusChem*, 2023, **16**(3), e202201875, DOI: 10.1002/CSSC.202201875.

72 W. G. Glasser, About Making Lignin Great Again—Some Lessons From the Past, *Front. Chem.*, 2019, **7**, 458843, DOI: 10.3389/fchem.2019.00565.

73 D. O. Abranches, M. A. R. Martins, L. P. Silva, N. Schaeffer, S. P. Pinho and J. A. P. Coutinho, Phenolic Hydrogen Bond Donors in the Formation of Non-Ionic Deep Eutectic Solvents: The Quest for Type V DES, *Chem. Commun.*, 2019, **55**(69), 10253–10256, DOI: 10.1039/C9CC04846D.

74 L. Chen, A. P. Van Muyden, X. Cui, Z. Fei, N. Yan, G. Laurenczy and P. J. Dyson, Lignin First: Confirming the Role of the Metal Catalyst in Reductive Fractionation, *JACS Au*, 2021, **1**(6), 729–733, DOI: 10.1021/jacsau.1c00018.

75 C. M. Hansen, *Hansen Solubility Parameters: A Users Handbook*, 2nd edn, 2007, pp. 113–123, DOI: 10.1201/9781420006834.

76 M. Mohan, K. Huang, V. R. Pidatala, B. A. Simmons, S. Singh, K. L. Sale and J. M. Gladden, Prediction of Solubility Parameters of Lignin and Ionic Liquids Using Multi-Resolution Simulation Approaches, *Green Chem.*, 2022, **24**(3), 1165–1176, DOI: 10.1039/D1GC03798F.

77 Y. Chen, Z. Yu, P. Rudnicki, H. Gong, Z. Huang, S. C. Kim, J. C. Lai, X. Kong, J. Qin, Y. Cui and Z. Bao, Steric Effect Tuned Ion Solvation Enabling Stable Cycling of High-Voltage Lithium Metal Battery, *J. Am. Chem. Soc.*, 2021, **143**(44), 18703–18713, DOI: 10.1021/jacs.1c09006.

78 E. West, A. S. Maclnnes and H. Hibbert, Studies on Lignin and Related Compounds. LXIX. Isolation of 1-(4-Hydroxy-3-methoxyphenyl)-2-propanone and 1-Ethoxy-1-(4-hydroxy-3-methoxyphenyl)-2-propanone from the Ethanolysis Products of Spruce Wood, *J. Am. Chem. Soc.*, 1943, **65**(6), 1187–1192, DOI: 10.1021/ja01246a048.

79 L. Brickman, W. L. Hawkins and H. Hibbert, Studies on Lignin and Related Compounds. XLVIII. Identification of Vanillin and Vanilloyl Methyl Ketone as Ethanolysis Products from Spruce Wood, *J. Am. Chem. Soc.*, 1940, **62**(8), 2149–2154, DOI: 10.1021/JA01865A063/ASSET/JA01865A063.FP.PNG_V03.

80 Z. Liu, H. Li, X. Gao, X. Guo, S. Wang, Y. Fang and G. Song, Rational Highly Dispersed Ruthenium for Reductive Catalytic Fractionation of Lignocellulose, *Nat. Commun.*, 2022, **13**(1), 1–11, DOI: 10.1038/s41467-022-32451-5.

81 T. Ren, S. You, Z. Zhang, Y. Wang, W. Qi, R. Su and Z. He, Highly Selective Reductive Catalytic Fractionation at Atmospheric Pressure without Hydrogen, *Green Chem.*, 2021, **23**(4), 1648–1657, DOI: 10.1039/D0GC03314F.

82 X. Xu, K. Wang, Y. Zhou, C. Lai, D. Zhang, C. Xia and A. Pugazhendhi, Comparison of Organosolv Pretreatment of Masson Pine with Different Solvents in Promoting Delignification and Enzymatic Hydrolysis Efficiency, *Fuel*, 2023, **338**, 127361, DOI: 10.1016/J.FUEL.2022.127361.

83 H. Fang, X. Xie, Q. Chu, W. Tong and K. Song, Modified 1,4-Butanediol Organosolv Pretreatment on Hardwood and Softwood for Efficient Coproduction of Fermentable Sugars and Lignin Antioxidants, *Bioresour. Technol.*, 2023, **376**, 128854, DOI: 10.1016/J.BIORTECH.2023.128854.

84 Y. Teramoto, S. H. Lee and T. Endo, Cost Reduction and Feedstock Diversity for Sulfuric Acid-Free Ethanol Cooking of Lignocellulosic Biomass as a Pretreatment to Enzymatic Saccharification, *Bioresour. Technol.*, 2009, **100**(20), 4783–4789, DOI: 10.1016/J.BIORTECH.2009.04.054.

85 Q. Song, F. Wang, J. Cai, Y. Wang, J. Zhang, W. Yu and J. Xu, Lignin Depolymerization (LDP) in Alcohol over Nickel-Based Catalysts via a Fragmentation–Hydrogenolysis Process, *Energy Environ. Sci.*, 2013, **6**(3), 994–1007, DOI: 10.1039/C2EE23741E.

86 X. Ouyang, X. Huang, J. Zhu, M. D. Boot and E. J. M. Hensen, Catalytic Conversion of Lignin in Woody Biomass into Phenolic Monomers in Methanol/Water Mixtures without External Hydrogen, *ACS Sustainable Chem. Eng.*, 2019, **7**(16), 13764–13773, DOI: 10.1021/acssuschemeng.9b01497.

87 W. Schutyser, S. Van Den Bosch, T. Renders, T. De Boe, S. F. Koelewijn, A. Dewaele, T. Ennaert, O. Verkinderen, B. Goderis, C. M. Courtin and B. F. Sels, Influence of Bio-Based Solvents on the Catalytic Reductive Fractionation of Birch Wood, *Green Chem.*, 2015, **17**(11), 5035–5045, DOI: 10.1039/C5GC01442E.

88 H. Zhou, X. Liu, Y. Guo and Y. Wang, Self-Hydrogen Supplied Catalytic Fractionation of Raw Biomass into Lignin-Derived Phenolic Monomers and Cellulose-Rich Pulps, *JACS Au*, 2023, **3**(7), 1911–1917, DOI: 10.1021/jacsau.3c00154.

89 J. K. Kenny, D. G. Brandner, S. R. Neefe, W. E. Michener, Y. Román-Leshkov, G. T. Beckham and J. W. Medlin, Catalyst Choice Impacts Aromatic Monomer Yields and Selectivity in Hydrogen-Free Reductive Catalytic Fractionation, *React. Chem. Eng.*, 2022, **7**(12), 2527–2533, DOI: 10.1039/D2RE00275B.

90 F. Brienza, K. Van Aelst, F. Devred, D. Magnin, B. F. Sels, P. Gerin, I. Cybulska and D. P. Debecker, Toward a Hydrogen-Free Reductive Catalytic Fractionation of Wheat Straw Biomass, *ChemSusChem*, 2023, **16**(13), e202300103, DOI: 10.1002/CSSC.202300103.

91 M. Verziu, A. Tirsoaga, B. Cojocaru, C. Bucur, B. Tudora, A. Richel, M. Aguedo, A. Samikannu and J. P. Mikkola, Hydrogenolysis of Lignin over Ru-Based Catalysts: The Role of the Ruthenium in a Lignin Fragmentation Process, *Mol. Catal.*, 2018, **450**, 65–76, DOI: 10.1016/J.MCAT.2018.03.004.

92 M. Takada and S. Saka, Characterization of Lignin-Derived Products from Japanese Cedar as Treated by Semi-Flow Hot-Compressed Water, *J. Wood Sci.*, 2015, **61**(3), 299–307, DOI: 10.1007/s10086-015-1464-0.

93 R. Hempfling and H. R. Schulten, Chemical Characterization of the Organic Matter in Forest Soils by Curie Point Pyrolysis-GC/MS and Pyrolysis-Field Ionization Mass Spectrometry, *Org. Geochem.*, 1990, **15**(2), 131–145, DOI: 10.1016/0146-6380(90)90078-E.

94 D. Tarmadi, Y. Tobimatsu, M. Yamamura, T. Miyamoto, Y. Miyagawa, T. Umezawa and T. Yoshimura, NMR Studies on Lignocellulose Deconstructions in the Digestive System of the Lower Termite Coptotermes Formosanus Shiraki, *Sci. Rep.*, 2018, **8**(1), 1–9, DOI: 10.1038/s41598-018-19562-0.

95 M. Sette, R. Wechselberger and C. Crestini, Elucidation of Lignin Structure by Quantitative 2D NMR, *Chem.–Eur. J.*, 2011, **17**(34), 9529–9535, DOI: 10.1002/CHEM.201003045.

96 R. Rinken, D. Posthuma and R. Rinaldi, Lignin Stabilization and Carbohydrate Nature in H-Transfer Reductive Catalytic Fractionation: The Role of Solvent Fractionation of Lignin Oil in Structural Profiling, *ChemSusChem*, 2023, **16**(3), e202201875, DOI: 10.1002/CSSC.202201875.

97 T. Vangeel, R. Smets, M. Van Der Borght and B. Sels, Depolymerisation–hydrogenation of condensed tannins as a strategy for generating flavan-3-ol monomers, *Green Chem.*, 2015, **25**(5), 1865–1874, DOI: 10.1039/D2GC04470F.

98 Y. Lu, Y. Zheng, R. He, W. Li and Z. Zheng, Selective Conversion of Lignocellulosic Biomass into Furan Compounds Using Bimetal-Modified Bio-Based Activated Carbon: Analytical Py-GC×GC/MS, *J. Energy Inst.*, 2020, **93**(6), 2371–2380, DOI: 10.1016/J.JOEI.2020.07.010.

99 C. Xu, E. Paone, D. Rodríguez-Padrón, R. Luque and F. Mauriello, Recent Catalytic Routes for the Preparation and the Upgrading of Biomass Derived Furfural and 5-Hydroxymethylfurfural, *Chem. Soc. Rev.*, 2020, **49**(13), 4273–4306, DOI: 10.1039/D0CS00041H.

100 K. Khallouk, A. Solhy, A. Kherbeche, E. Dubreucq, L. Kouisni and A. Barakat, Effective Catalytic Delignification and Fractionation of Lignocellulosic Biomass in Water over Zn3V2O8 Mixed Oxide, *ACS Omega*, 2020, **5**(1), 304–316, DOI: 10.1021/acsomega.9b02159.

101 S. Cheng, I. D'cruz, M. Wang, M. Leitch and C. Xu, Highly Efficient Liquefaction of Woody Biomass in Hot-Compressed Alcohol-Water Co-Solvents, *Energy Fuel.*, 2010, **24**(9), 4659–4667, DOI: **10.1021/ef901218w**.

102 L. Segal, J. J. Creely, A. E. Martin and C. M. Conrad, An Empirical Method for Estimating the Degree of Crystallinity of Native Cellulose Using the X-Ray Diffractometer, *Text. Res. J.*, 1959, **29**(10), 786–794, DOI: **10.1177/004051755902901003**.

103 H. Kargarzadeh, I. Ahmad, I. Abdullah, A. Dufresne, S. Y. Zainudin and R. M. Sheltami, Effects of Hydrolysis Conditions on the Morphology, Crystallinity, and Thermal Stability of Cellulose Nanocrystals Extracted from Kenaf Bast Fibers, *Cellulose*, 2012, **19**(3), 855–866, DOI: **10.1007/s10570-012-9684-6**.

104 H. Li, X. Cai, Z. Wang and C. Xu, Cost-Effective Production of Organosolv Lignin from Woody Biomass Using Ethanol-Water Mixed Solvent at Mild Conditions, *J. Supercrit. Fluids*, 2020, **158**, 104745, DOI: **10.1016/J.SUPFLU.2019.104745**.

105 R. A. Sheldon, Metrics of Green Chemistry and Sustainability: Past, Present, and Future, *ACS Sustainable Chem. Eng.*, 2018, **6**(1), 32–48, DOI: **10.1021/acssuschemeng.7b03505**.